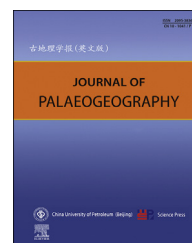




Available online at www.sciencedirect.com

ScienceDirect

journal homepage: <http://www.journals.elsevier.com/journal-of-palaeogeography/>



Lithofacies palaeogeography and sedimentology

Hyperpycnal littoral deltas: A case of study from the Lower Cretaceous Agrio Formation in the Neuquén Basin, Argentina

Ainara Irastorza ^{a,b,*}, Carlos Zavala ^{a,c},
Débora Mical Campetella ^{e,f}, Martín Turienzo ^{a,b},
Daniela Olivera ^{a,b}, Florencia Peralta ^b, Maite Irastorza ^a,
Paula Martz ^d

^a Dpto. de Geología, Universidad Nacional Del Sur (UNS), Bahía Blanca 8000, Argentina

^b Instituto Geológico Del Sur (INGEOSUR), Universidad Nacional Del Sur (UNS)-CONICET, Bahía Blanca 8000, Argentina

^c GCS Argentina SRL, Molina Campos 150, Bahía Blanca 8000, Argentina

^d Universidad Nacional Del Sur, Bahía Blanca 8000, Argentina

^e Universidad Nacional de Río Negro. Instituto de Investigación de Paleobiología y Geología, General Roca 8332, Río Negro, Argentina

^f Consejo Nacional de Investigaciones Científicas y Técnicas (CONICET), Instituto de Investigaciones en Paleobiología y Geología, General Roca 8332, Río Negro, Argentina

Abstract Recent advances in the understanding of deltaic deposits provide new tools for the study and analysis of deltaic deposits in shallow epicontinental seas. After the introduction of sequence stratigraphic concepts, meter-scale coarsening and thickening upward successions have been considered as “para-sequences” originated by high-frequency sea-level changes. Nevertheless, recent studies enhanced the importance of wave-aided low-dense hyperpycnal flows in transporting fine-grained sediments in shallow shelfal areas. These poorly-known (and at the same time very common) types of delta, known as hyperpycnal littoral deltas (HLD), develop very low gradient progradational units, controlled by changes in the sediment supply instead of sea level changes. These small-scale progradational units are very common in shallow epicontinental seas like the Lower Cretaceous Agrio Formation in the Neuquén Basin. This study provides a first detailed analysis of hyperpycnal littoral deltas from the Agua de la Mula Member (upper Hauterivian–lower Barremian) of the Agrio Formation. This unit has been studied in three locations near Bajada del Agrio locality in the central part of the Neuquén Basin, Argentina. Six sandy facies, three heterolithic facies, three muddy facies and four calcareous facies were recognized. From facies analysis, three facies associations could be determined, corresponding to offshore/prodelta, distal ramp delta and proximal ramp delta. The three stratigraphic sections discussed in this study are internally composed of several small-scale sequences showing a coarsening and thickening upward pattern, transitionally going from muddy to sandy wave-dominated facies, and ending with calcareous bioclastics levels on top. These small-scale sequences are interpreted as delta

* Corresponding author.

E-mail address: airastorza@ingeosur-conicet.gob.ar (A. Irastorza).

Peer review under responsibility of China University of Petroleum (Beijing).

<https://doi.org/10.1016/j.jop.2021.11.004>

2095-3836/© 2021 The Authors. Published by Elsevier B.V. on behalf of China University of Petroleum (Beijing). This is an open access article under the CC BY-NC-ND license (<http://creativecommons.org/licenses/by-nc-nd/4.0/>).



front deposits of wave-influenced hyperpycnal littoral deltas, punctuated by calcareous intervals accumulated during periods of low sediment supply. It is interpreted that the development of hyperpycnal littoral deltas could have been facilitated by a decrease in sea water salinity related to an increasing runoff.

Keywords Deltas, Hyperpycnal littoral deltas, Prograding sequences, Agua de la Mula Member, Neuquén Basin

© 2021 The Authors. Published by Elsevier B.V. on behalf of China University of Petroleum (Beijing). This is an open access article under the CC BY-NC-ND license (<http://creativecommons.org/licenses/by-nc-nd/4.0/>).

Received 31 May 2021; revised 21 July 2021; available online 13 November 2021

1. Introduction

The term “delta” was introduced by the Greek philosopher Herodotus (490 BC), according to the triangular shape (similar to the Greek letter “delta”) of the deposits accumulated close to the Nile River mouth. In recent decades, these systems have been studied and classified in several ways, considering the dominant diffusion process at coastal areas, the grain-size of the supplied sediments and the density contrast between the incoming flow and the receiving water body (Bates, 1953; Wright and Coleman, 1973; Galloway, 1975; Postma, 1995; Bhattacharya, 2006). However, there is a tendency to simplify deltaic sedimentation as littoral deltas. Littoral deltas are formed by the rapid loss of flow capacity and competence of a river discharge at coastal areas, resulting in the accumulation of shallow mouth bars. Nevertheless, there are diverse variables (operating at regional and local scales) that can affect the development and evolution of these complex systems (Zavala *et al.*, 2021). Some factors to consider are the slope at the coastal area, autocyclic and allocyclic processes (tectonism, eustatic changes and climatic conditions) and density of fluvial discharges. Incoming flows, derived from fluvial discharges, can be highly variable (in terms of volume and sediment concentration, sediment grain size, water density and turbidity, etc.) and give rise to different deltaic deposits (Bates, 1953; Mulder and Syvitski, 1995; Mutti *et al.*, 1996; Mulder and Alexander, 2001; Mulder *et al.*, 2003; Zavala *et al.*, 2021).

In the Neuquén Basin, the Agrio Formation (late Valanginian–early Barremian) represents the third transgression from the paleo-Pacific Ocean. It is divided into three members: Pilmatué, Avilé and Agua de la Mula (Weaver, 1931; Leanza *et al.*, 2001). This work focusses on the Agua de la Mula Member, which has been interpreted as accumulating in a homocline, low-gradient ramp system with mixed siliciclastic–

carbonate components, depositing under fair-weather and storm wave influence (Spalletti *et al.*, 2001a, 2001b; Lazo *et al.*, 2005; Sagasti, 2005; Comerio *et al.*, 2018, 2019; Fernández *et al.*, 2019). The aim of this study is 1) to perform an analysis of facies and facies associations of three sedimentological-stratigraphic sections, and 2) to propose a new depositional model for Agua de la Mula Member in the study area related to hyperpycnal littoral deltas.

2. Geological setting

2.1. Tectonostratigraphic setting

The Neuquén Basin is located at the western margin of South America between 32° and 40° south latitude (Fig. 1a). It has been defined as a large ensialic backarc basin originated as a result of the thermal-tectonic collapse behind a stationary magmatic arc during the Late Triassic (Mpodozis and Ramos, 1989). The Neuquén Basin is bounded by the Sierra Pintada System to the northeast, the North Patagonian Massif to the southeast, and by the Andean magmatic arc to the west. During the Early Jurassic–late Early Cretaceous the Neuquén Basin was flooded by the paleo-Pacific Ocean throughout narrow passages along an active volcanic arc (Howell *et al.*, 2005). This marine connection was punctuated with some periods of disconnection related to relative sea-level variations (Legarreta and Uliana, 1991; Mutti *et al.*, 1994a; Zavala *et al.*, 2006) associated with tectonic and eustatic changes.

The Neuquén Basin records at least 220 m.y. of basin subsidence with a preserved stratigraphic column of up to 7000 m, mainly accumulated during the Jurassic and Cretaceous (Howell *et al.*, 2005). Deposits are chiefly clastic (shallow marine and continental), although some mixed carbonates, reef limestones and evaporites are locally recognized. Along the Neuquén Basin

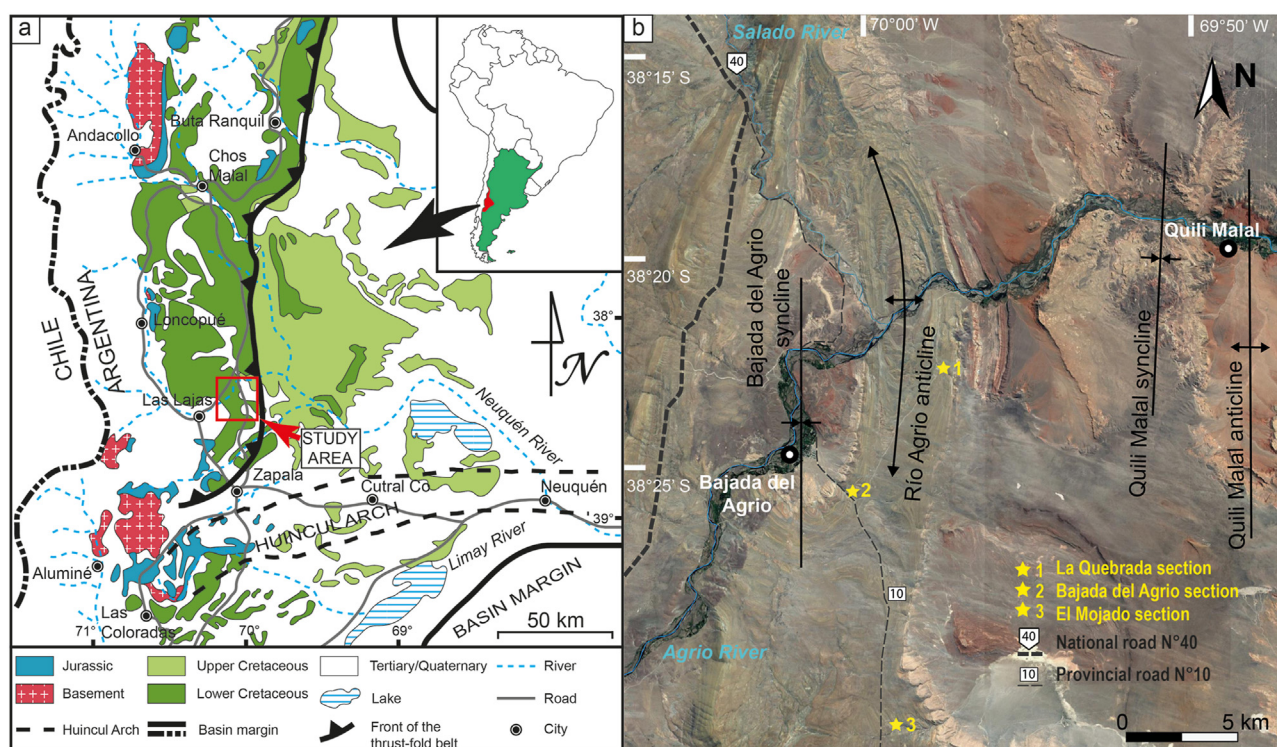


Fig. 1 a Simplified geological map of the Neuquén Basin indicating the location of the study area. Modified from Zavala *et al.*, 2006; b Detailed satellite image of the study area showing main structural elements and the three stratigraphic columns here analyzed.

fill, three main depositional stages can be recognized, corresponding to (1) syn-rift, (2) post-rift, and (3) foreland basin stage (Uliana *et al.*, 1989; Vergani *et al.*, 1995; Howell *et al.*, 2005; Kietzmann and Folguera, 2020). The first stage occurred during the Late Triassic–Early Jurassic, controlled by NW–SE normal faults associated to rifting at the western margin of Gondwana (Uliana *et al.*, 1989; Vergani *et al.*, 1995; Franzese and Spalletti, 2001; Howell *et al.*, 2005). This phase includes continental, marine and volcanoclastic sediments assigned to the Precuyo Group (Gulisano, 1981; Gulisano and Gutiérrez Pleimling, 1995; Franzese and Spalletti, 2001). The second stage (Early Jurassic to Early Cretaceous) corresponds to a post-rift stage. Initially the sedimentation was influenced by the topography inherited from the previous syn-rift systems (Vergani *et al.*, 1995; Burgess *et al.*, 2000). Back-arc subsidence results in the flooding of the basin from the proto-Pacific Ocean (Spalletti *et al.*, 2000; Macdonald *et al.*, 2003) with a series of transgressive–regressive cycles that accumulated continental and marine deposits in isolated or partially connected depocenters (Arregui *et al.*, 2011). These deposits correspond to the Cuyo, Lotena and Mendoza groups (Howell *et al.*, 2005). The foreland basin stage (Late Cretaceous to Cenozoic), includes a reorganization of

the Pacific Plate and a decrease in the subduction angle, that resulted in a compressional tectonic regime (Vergani *et al.*, 1995; Ramos and Folguera, 2005; Ramos and Kay, 2006) that caused fold and thrust belts along the western region of the basin. During this stage, a marine to continental succession with a highly variable thickness filled the Neuquén Basin (Bajada del Agrio and Neuquén groups) (Legarreta and Uliana 1991, 1999; Vergani *et al.*, 1995).

2.2. The Agrio Formation

The Agrio Formation (Weaver, 1931) is the uppermost unit of the Mendoza Group. According to ammonoid, nannoplankton and palynomorph studies calibrated with U–Pb zircon ages, the ages of the Agrio Formation ranges from late early Valanginian to late Hauterivian (Aguirre-Urreta *et al.*, 2017, 2019). This unit is composed of three members (from base to top): Pilmatué, Avilé, and Agua de la Mula (Weaver, 1931; Leanza *et al.*, 2001). Both the Pilmatué and Agua de la Mula members are shallow marine in origin and have been interpreted as accumulating in a storm-dominated shallow marine environment, characterized by a mixed siliciclastic and carbonate sedimentation (Spalletti *et al.*, 2001a). On the contrary, the

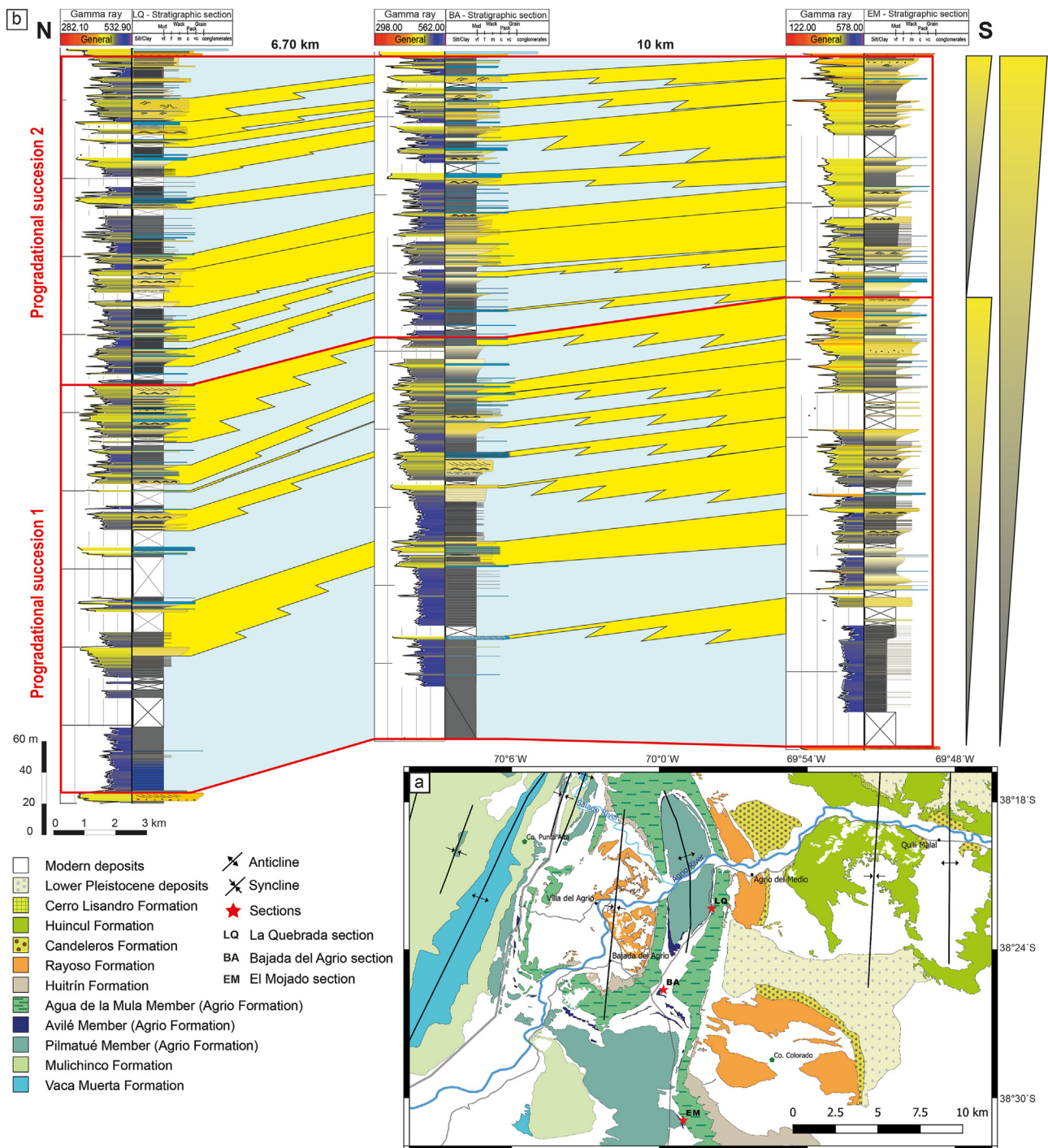


Fig. 2 a Geological map of the study area, in the frontal part of the Agrio fold-thrust belt (from Irastorza et al., 2019); b Correlation panel of measured stratigraphic sections in the Agua de la Mula Member in La Quebrada, Bajada del Agrio and El Mojado locations. Note that the entire member shows an overall progradational trend, where two internal progradational successions (1 and 2) can be recognized. Each progradational succession is internally composed of several high-frequency progradational cycles or “parasequences”.

Avilé Member is composed of sandstones, minor shales and evaporites of fluvial, lacustrine and aeolian origin (Guliano and Gutiérrez Pleimling, 1988; Veiga and Vergani, 1993).

This paper focused on unravelling the sedimentology and depositional environments of the Agua de la Mula Member in central areas of the Neuquén Basin (Fig. 1). This member starts after an important

transgressive event, dated as mid-Hauterivian (Aguirre-Urreta and Rawson, 1997), and is composed of dark mudstones, sandstones and bioclastic limestones. This member is unconformably overlain by the Huitrín Formation, which is the first unit of the Bajada del Agrio Group.

3. Methods

This sedimentological and stratigraphic study is focused on the analysis of outcrops from the Agua de la Mula Member (Agrio Formation) located near the Bajada del Agrio locality (Fig. 1b). These exposures occur around the Río Agrio anticline, which constitutes the deformation front of the southern Agrio fold-thrust belt. During field surveys, numerous bedding attitude data were also acquired, allowing the construction of a regional map of the study area using the QGIS 2.18.15 software (Fig. 2a) and a balanced structural cross-section supported by 2D seismic data (Irastorza *et al.*, 2019). Three detailed sedimentary sections were measured in the Agua de la Mula Member, from the Avilé Member up to the base of the Huitrín Formation. These sections were carefully described and measured bed-by-bed using Brunton compass, Jacob's staff, hydrochloric acid, a photographic camera and a handheld Gamma Ray counter. During the description, special care was taken in the observation of lithology and texture, primary sedimentary structures, bed geometries and relation between beds and fossil content. These observations allowed setting up a detailed facies analysis, from where main sedimentary processes and related depositional elements were recognized. A number of rock samples for petrological (41 samples) and palynological analysis (8 samples) were collected. The measured sedimentological sections have thicknesses ranging between ~440 and 483 m and were first drawn in a 1:200 scale with the scope of characterizing sedimentary facies and facies associations, and their relationship with field Gamma Ray data. These sections were later drawn in a 1:2000 scale in order to facilitate the regional correlation of depositional sequences. Eight palynological samples were studied. The physical and chemical extraction of the palynological matter (PM) was carried out at the Palynological Laboratory of the Instituto Geológico del Sur (INGEOSUR)/Universidad Nacional del Sur (UNS)-Bahía Blanca. All samples were prepared according to standard non-oxidative palynological techniques, which involved treatments with hydrochloric and hydrofluoric acids. This residue was sieved using a 10- μ m mesh according to Tyson (1995) and a slide was

prepared. The slides were examined using a transmitted white-light microscope (Olympus BX40). At least 500 particles were point-counted per slide using a 40 \times objective for the second slide.

4. Results

The Agua de la Mula Member was measured and analyzed in three locations: Bajada del Agrio, La Quebrada and El Mojado. The Bajada del Agrio and La Quebrada sections are located at both flanks of the Río Agrio anticline, while the El Mojado section is located south of this anticline, near provincial road N°10 (Fig. 1b). Muddy, heterolithic, sandy and calcareous facies have been identified, which occur in several facies associations. Within the studied sections, biogenic structures are in general poorly abundant and are characterized by a low to moderate diversity and abundance of trace fossils.

The stratigraphic sections were correlated with an N–S orientation (Fig. 2b). In the figure, different orders of cyclicity can be recognized (megasequences, sequences, and elementary depositional sequences) with thickening and coarsening-upward arrangements. This gives the entire sequence a prograding characteristic.

4.1. Facies

The facies nomenclature adopted in this work is based on a descriptive procedure firstly introduced by Miall (1978) in which letters represent macroscopic characteristics of the rock body. In this classification, the first letter (capital) represents the main lithology and the following letters indicate additional characteristics as grain size, dominant sedimentary structure and accessories. As an example, facies SfM refers to a massive fine-grained sandstone. Special attention was paid in trying to clearly differentiate the description and interpretation of each facies.

4.1.1. Sandy facies

4.1.1.1. Facies SfM. Description: Facies SfM is composed of massive and diffuse parallel laminated well-sorted medium to very fine-grained sandstones, with a greyish to pale yellow colouring. Individual beds range from a few centimeters up to ~3 m and show tabular to lenticular geometry. Facies SfM is commonly draped at the top with ripple bedforms composing straight to sinuous symmetrical to slightly-asymmetrical and interference forms, with no internal structure (Fig. 3a). Articulated, disarticulated and

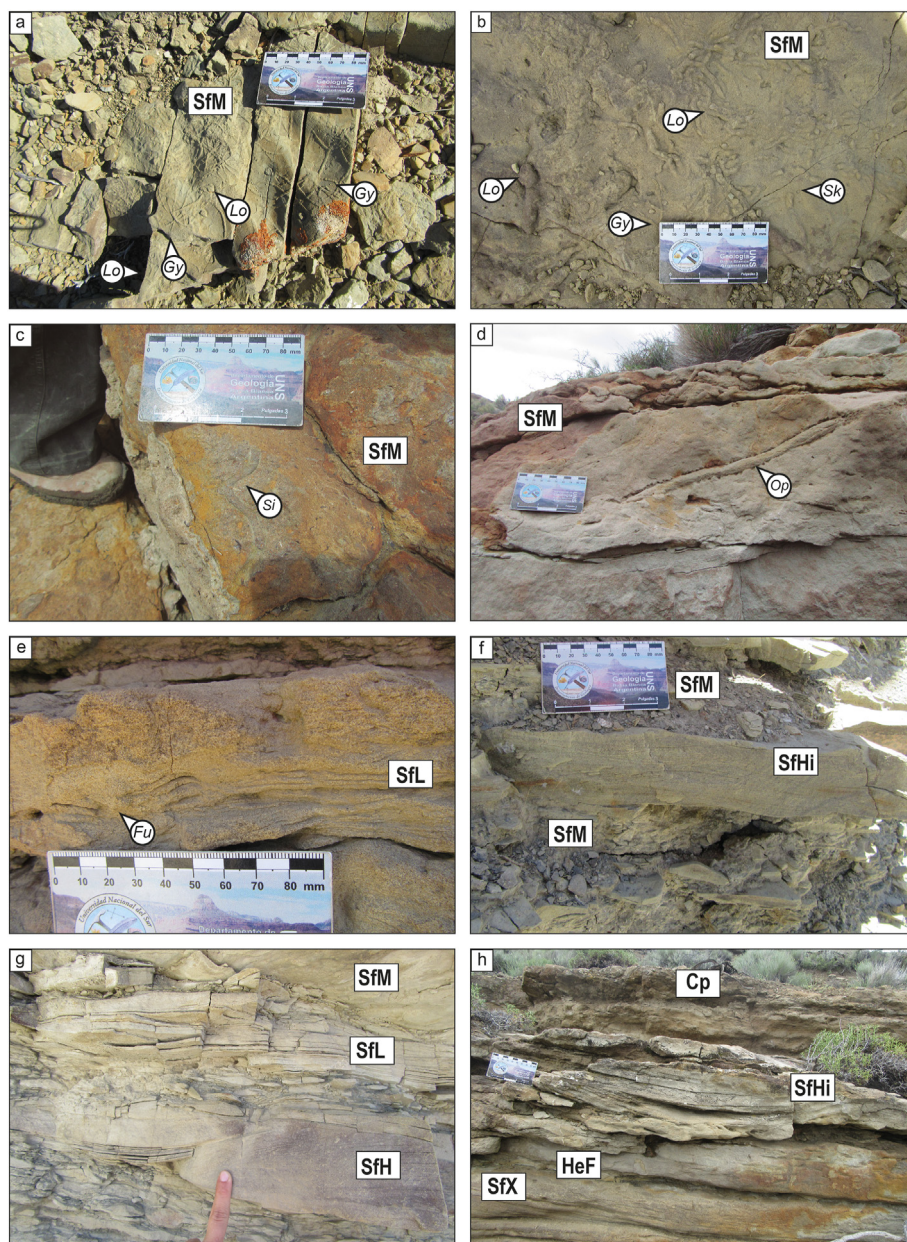


Fig. 3 Sandy facies. **a** Interference ripples at the top of massive sandstones with trace fossils of *Gyrochorte* (Gy) and *Lockeia* (Lo); **b** Bioturbated massive sandstones with *Gyrochorte* (Gy), *Lockeia* (Lo) and *Skolithos* (Sk); **c** *Sinusichnus* trace (Si) in massive sandstones with fragmented valves; **d** *Ophiomorpha* (Op) traces in massive sandstones; **e** *Fugichnia* (Fu) in laminated sandstones; **f** Massive sandstones interbedded with sandstones with isotropic hummocky cross-stratification (HCS); **g** Transitional passage between laminated, HCS and massive sandy facies; **h** Thickening-upward cycles composed of asymptotic cross-bedding sandstones, flaser heterolithic sandstones, isotropic HCS sandstones, and limestones (in sharp contact). Cp: Packstone calcareous facies; HeF: Flaser heterolithic facies; SfH: Hummocky sandy facies; SfHi: Isotropic hummocky sandy facies; SfL: Laminated fine-grained sandy facies; SfM: Massive fine-grained sandy facies; SfX: Asymptotic and trough cross-bedding sandy facies.

fragmented valves, small gastropods, serpulids and oolites are also common. Locally, this facies shows dispersed carbonaceous remains and micas. Small clay chips are common, sometimes grouped toward the base or top of sandstone bodies. Deformation and fluid escape structures are common in massive sandstones.

In general, these sandstones are calcareous and compose thickening- and coarsening-upward cycles, in combination with other sandy facies. Moderate to high bioturbation is often observed, with forms of *Gyrochorte*, *Lockeia*, *Ophiomorpha*, *Sinusichnus* and *Skolithos* (Fig. 3a–d).

Interpretation: The origin of massive sandstones is related to the progressive aggradation of sand grains accumulated at the base of long-lived sustained turbulent flows with high suspended load (Sanders, 1965; Kneller and Branney, 1995; Camacho *et al.*, 2002; Sumner *et al.*, 2008). Experimental studies demonstrated that turbulent flows with fallout rates higher than 0.44 mm/s could inhibit the formation of primary sedimentary structures resulting in massive sandstone bodies (Banerjee, 1977; Arnott and Hand, 1989; Sumner *et al.*, 2008). Massive beds accumulate in a zone of aggrading transition between the deposit and the overpassing flow, characterized by a high sediment concentration associated with water escape (Kneller and Branney, 1995). Wave-ripple bedforms on top would suggest the post-depositional reworking by bi-directional currents. In general, this facies is characterized by a well-sorted fabric, due to the maximum available grain size in a turbulent suspension is limited by flow velocity and competence (Zavala and Pan, 2018). Bioclastic levels in this facies could suggest gradual changes in flow conditions, characterized by internal erosion, transport and deposition of bioclasts as bedload (traction-saltation). As flow velocity gradually wanes, massive sands continue to be accumulated by fallout from a sustained turbulent flow. The localized occurrence of *Ophiomorpha* and *Skolithos* indicates the presence of opportunistic, suspension feeding organisms and reflects high energy conditions and suspended load developed after the deposition of sandstone levels (Carmona, 2005; Buatois and Mángano, 2011). The presence of *Gyrochorte*, *Lockeia* and *Sinusichnus* related to wave-ripples bedforms are assigned to deposit-feeding organisms that reflected benthic food availability, low to moderate energy and high turbidity in the water column (MacEachern *et al.*, 2005; Buatois and Mángano, 2011; Soares *et al.*, 2020; Wetzel *et al.*, 2020).

4.1.1.2. Facies SfL. **Description:** The SfL facies consists of medium- to fine-grained well-sorted sandstones with parallel lamination and greyish to light yellow colouring. Individual beds range from a few centimeters up to ~1.5 m. This facies composed tabular beds, lying on a sharp to transitional base and, exceptionally, infilling channel fill bodies lying on erosional bases. Facies SfL appears in close association with SfM, SfR, SfH and HeW facies. Symmetrical straight to sinuous ripples are often observed as bedforms on top of laminated beds. Carbonaceous remains and micas are commonly found along laminae. Bioclasts (disarticulated and fragmented valves) and clay chips are also common at the bottom of sandstone bodies. Ball and pillow structures are frequent at the

base of sandstone beds. Bioturbation has been locally recognized, mostly in the form of escape structures (*Fugichnia*) (Fig. 3e).

Interpretation: The origin of planar lamination has been related to different depositional processes, generally associated with upper flow regime (Simons *et al.*, 1965; Allen, 1984). Nevertheless, flume experiments suggest that planar lamination associated with massive sandstone indicates deposition of sands by fallout from sustained turbulent flows with sedimentation rates lower than 0.44 mm/s (Sumner *et al.*, 2008). Sanders (1965) documented a lateral transition between planar lamination and climbing ripples, implying a common origin of these structures to traction-plus-fallout processes. For this reason, in this paper, laminated sandstones are related to fallout processes from turbulent suspensions. Carbonaceous remains were probably part of the overpassing turbulent flow, deposited together with micas along a progressively aggradational depositional surface. Escape trace fossils evidence relatively high rates of fallout in a stressed environment (Buatois and Mángano, 2011).

4.1.1.3. Facies SfH (including SfHi and SfHa).

Description: Facies SfH is composed of greyish to pale yellow medium- to fine-grained sandstones with hummocky cross-stratification. Two subfacies can be recognized, corresponding to SfHi (isotropic HCS) and SfHa (anisotropic HCS). Beds are tabular or irregular, with a thickness ranging from a few centimeters up to 20–50 cm. Lower boundaries are generally sharp or erosional. This facies commonly shows fluid escape structures. Fragmented valves and clay chips (at the bottom and/or top of beds) can also be found. Sometimes, facies SfH is draped at the top with ripple bedforms composing straight to sinuous symmetrical to slightly asymmetrical forms, with no internal sedimentary structures. Lamina sets are often separated by onlapping relations. In general, facies SfH is associated with facies SfM and SfL (Fig. 3f and g).

Interpretation: Hummocky cross-stratification (HCS) has usually been used as a criterion for the recognition of shoreface deposits punctuated by storm events (Barron, 1989; Harms *et al.*, 1975), being characteristic of tempestite beds (Dott and Bourgeois 1982, 1983; Walker *et al.*, 1983). However, some authors related the origin of this structure to the occurrence of both unidirectional and oscillatory components at a certain depth, independent of surface storm waves (Allen, 1984; Allen and Pound, 1985; Southard, 1991; Mutti *et al.*, 1994b; Morsilli and Pomar, 2012). Mutti *et al.* (1994a) stated that the oscillatory component could result from the putting in motion of a shallow standing body of water, produced

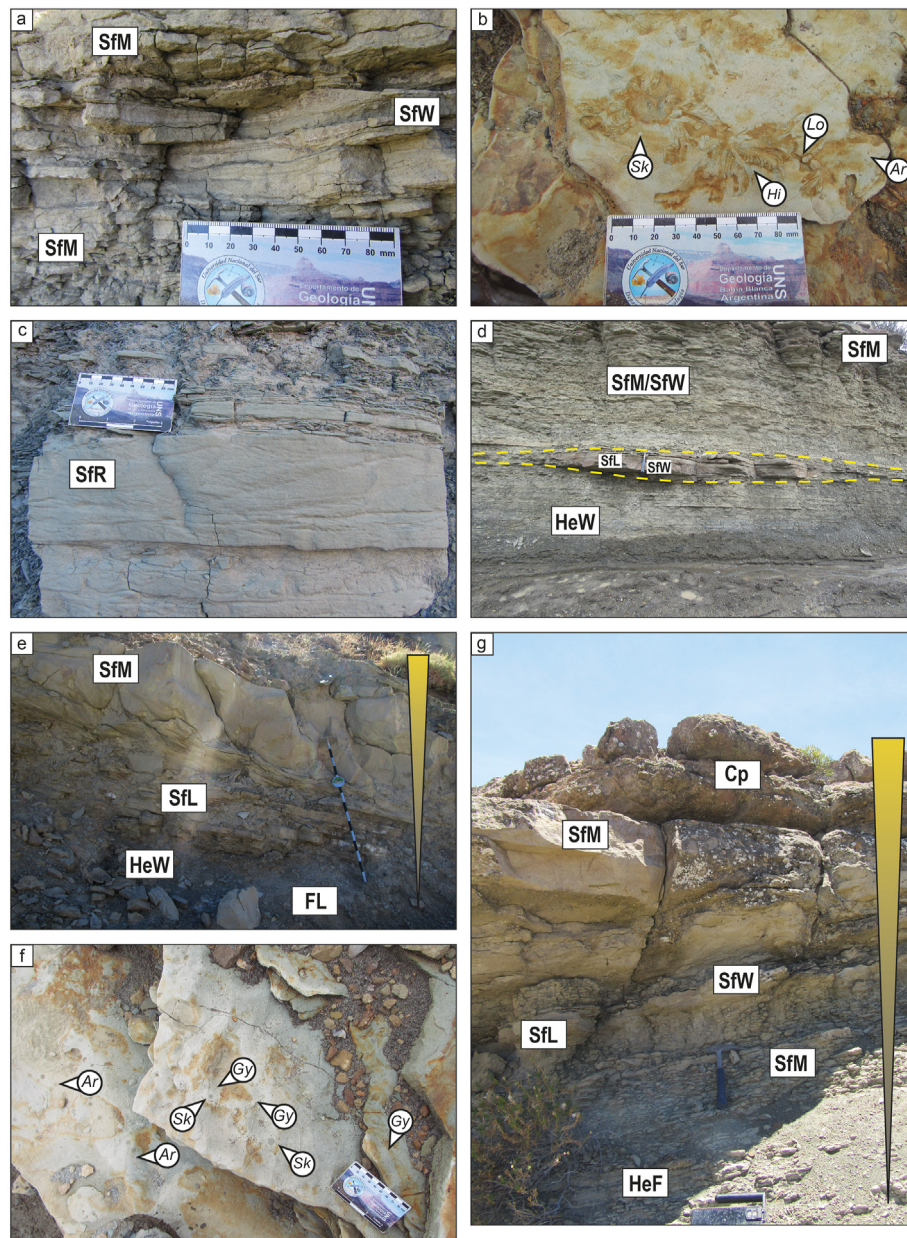


Fig. 4 Sandy, heterolithic and muddy facies. **a** Massive sandy facies (SfM) interbedded with wave truncated sandstones (SfW). **b** Trace fossils recognized at the top of wave truncated sandy facies (SfW) (*Arenicolites* (Ar), *Hillichnus* (Hi), *Lockeia* (Lo), and *Skolithos* (Sk)). **c** Climbing ripples sandy facies (SfR). **d** Thickening- and coarsening-upward cycle with wavy heterolithic (HeW), laminated (SfL) and wave truncated sandstones (SfW) with channelized geometry and interbedded with massive/wave truncated sandstone (SfM–SfW). **e** Thickening- and coarsening-upward succession of laminated mudstone (FL) followed by wavy heterolithic deposits (HeW), and laminated and massive sandstone (SfL–SfM). Fluid escape structures are observed in massive sandstones (SfM) at the top of the cycles. **f** Bioturbation at the top of heterolithic facies (*Arenicolites* (Ar), *Gyrochorte* (Gy), and *Skolithos* (Sk)). **g** Thickening- and coarsening-upward succession showing transitional contacts between flaser heterolithics (HeF), massive sandstones (SfM), laminated sandstones (SfL), and wave truncated sandstones (SfW), with limestones (Cp) on top.

by the sudden entrance of a considerable volume of water during river floods (hyperpycnal discharges). Consequently, isotropic HCS (facies SfHi) can also develop in non-wave-dominated settings, as being documented by Zavala *et al.* (2006) at the lacustrine Rayoso Formation (Albian). The last could

conveniently explain the common occurrence of wave reworking only at the top of sandstone bodies, and not in the associated deposits dominated by mud deposition. Some recent experiments (Dumas *et al.*, 2005; Dumas and Arnott, 2006) show that HCS can be generated under moderate to high oscillatory

velocities (higher than 50 cm/s) and low unidirectional velocities (lower than 10 cm/s). This facies can be regarded as the product of internal waves either in lacustrine or marine environments, often associated with hyperpycnal and intrabasinal turbidity flows (Morsilli and Pomar, 2012).

Anisotropic HCS structures (facies SfHa) are interpreted as deposited from oscillatory-dominant combined flows associated with a stronger unidirectional flow component (Arnott and Southard, 1990; Mutti et al., 1996) in confined areas of stream flows. Some authors consider anisotropic HCS as a sedimentary structure with transitional characteristics between low-angle cross-stratification and ideal hummocky cross-stratification (Midtgaard, 1996).

4.1.1.4. Facies SfX. **Description:** This facies is composed of greyish to pale yellow medium- to fine-grained well-sorted sandstones with asymptotic and trough cross-bedding (Fig. 3h). Individual beds are up to 20 cm thick and have a tabular geometry and sharp bases. Dispersed carbonaceous remains are found along foresets, often associated with silty levels.

Interpretation: According to Harms et al. (1982), the origin of cross-bedding structures is related to the migration of straight (2D) and sinuous (3D) dunes. Asymptotic bedding suggests the collapse of suspended load at the lower lee-side of dune foresets, thus indicating an origin related to sustained turbulent flows with high suspended load (Midtgaard, 1996).

4.1.1.5. Facies SfW. **Description:** Facies SfW is composed of greyish to light yellow fine- to medium-grained sandstones with symmetrical (wave) ripples associated with wave truncation structures. Beds are tabular or irregular with a thickness of a few centimeters (up to 30 cm), often infilling channelized surfaces, or encased in wavy heterolithic facies. Small, fragmented valves can also be found. In general, facies SfW is associated with facies SfM, SfL and HeW (Fig. 4a). Trace fossils of *Arenicolites*, *Gyrochorte*, *Hillichnus*, *Lockeia* and *Skolithos* are found (Fig. 4b).

Interpretation: According to Campbell (1966), truncated wave ripple laminae form when a vortex of sand in suspension forms over each ripple crest as each wave crest passes on the sea bottom. The deposition is related to bidirectional wave's motion that distributes the sand across the ripple crest and into adjacent troughs. Each set can be truncated by the overlying set of wave-ripple laminae. Symmetrical ripples are interpreted as resulting from pure oscillatory ripples (Harms, 1969). *Arenicolites* and *Skolithos* trace fossils correspond to opportunistic suspension feeding

organism and occur in periods with high energy and suspended load during the re-work of sediments by waves (Buatois and Mángano, 2011), whereas *Gyrochorte*, *Hillichnus* and *Lockeia* are developed by deposit-feeding organisms that colonize the substrate during low to moderate energy and benthic food availability periods between low to moderate energy events (Bromley et al., 2003; Buatois and Mángano, 2011; López Cabrera et al., 2019; Wetzel et al., 2020).

4.1.1.6. Facies SfR. **Description:** This facies is composed of greyish to pale yellow medium- to fine-grained well-sorted sandstones with climbing ripples. Each bed has a thickness of a few centimeters up to 30 cm with a tabular geometry (Fig. 4c). Carbonaceous remains and micas usually appear covering ripple foresets. This facies appears associated with SfM and SfL facies.

Interpretation: Climbing ripples are generated by traction-plus-fallout processes from sustained turbulent flows with a high sedimentation rate (Jopling and Walker, 1968; Mulder and Alexander, 2001; Sumner et al., 2008) and an average flow velocity between 15 and 25 cm/s (Ashley et al., 1982). Laminated and climbing ripple facies often grade laterally and vertically between them (Sanders, 1965; Zavala et al., 2006), indicating a common origin related to traction-plus-fallout processes. The transition from laminated to climbing rippled sandstones suggests a decrease in flow velocity (Sanders, 1965) with a substantial increase in the fallout rate as the flow loses capacity. In consequence, cyclic changes between laminated facies and climbing ripple facies indicate fluctuations in the velocity of the overpassing turbulent flow (Zavala et al., 2006).

4.1.2. Heterolithic facies

In this category are included deposits composed of different proportions of sand-silt components: facies HeF, HeW and HeL (Fig. 4d–g).

Facies HeF is composed of massive and diffuse parallel-laminated well-sorted medium to very fine-grained sandstones (composing up to 80% of the facies) locally draped or interbedded with thin continuous or discontinuous levels of black massive mudstone intercalations, forming flaser bedding. In general, this facies grades into massive or laminated sands.

The HeW facies is made up of massive or laminated black mudstones interbedded with well-sorted massive to diffuse parallel sandstones, forming wavy bedding. Sandstone beds have tabular geometry and thickness of 2–10 cm. Sometimes, these beds show erosive bases

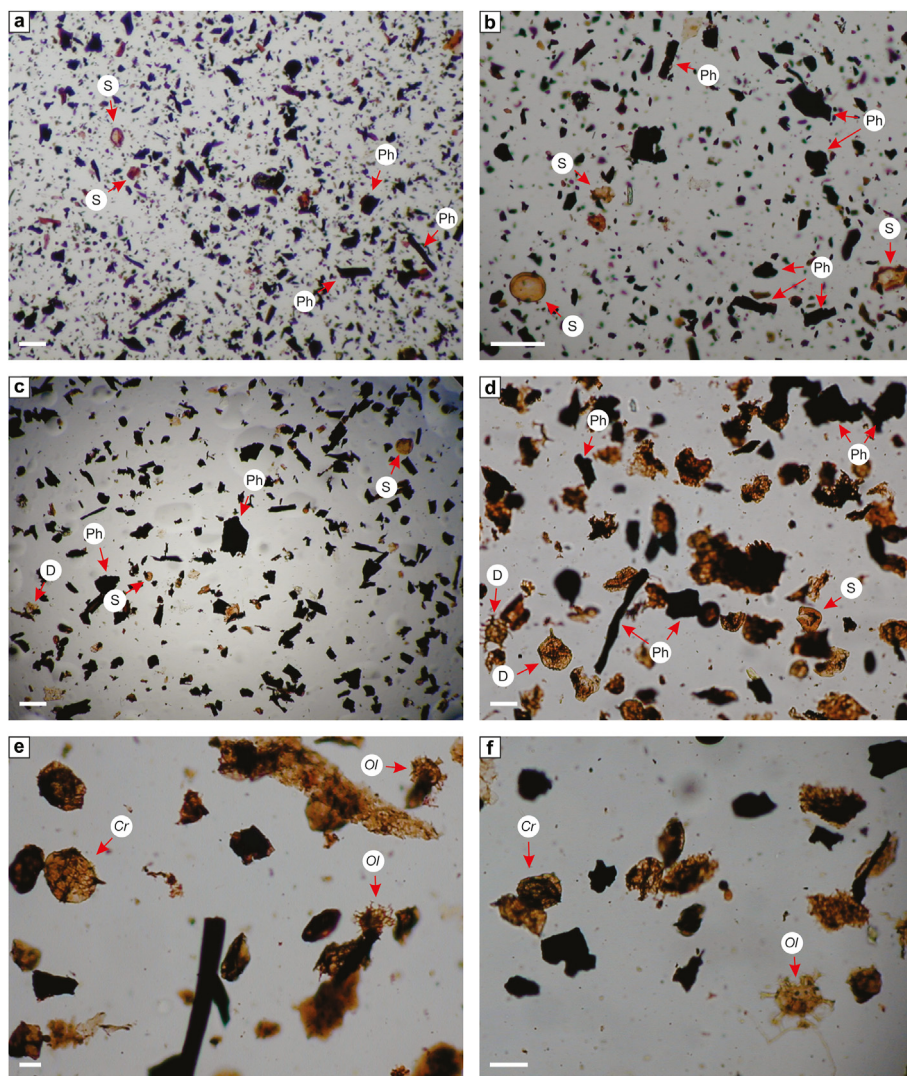


Fig. 5 Palynological organic matter from the Agua de la Mula Member (Agrio Formation) at the Bajada del Agrio section. Scale bar: 50 microns. Ph: Phytoclasts; S: Sporomorph; D: Dinoflagellate cysts; Ol: *Oligosphaeridium*; Cr: *Cribroperidinium*. **a** Palynofacies A, highly dominated by terrestrially-derived phytoclasts. Palynomorphs and AOM are subordinated. Palynomorph assemblages are mostly composed by terrestrially-derived palynomorphs (sporomorphs). **b** Phytoclast-dominated palynofacies A. **c** Sub-palynofacies B1, mostly composed by phytoclasts and palynomorphs. Sporomorphs (pollen grains and spores) dominate the palynomorph assemblages, being proportions of dinoflagellate less than 13%. **d** Sub-palynofacies B2, mostly composed by phytoclasts and palynomorphs. Sporomorphs dominate the palynomorph assemblages and dinoflagellate cysts reach up to 26%. **e** and **f** Species of *Oligosphaeridium* and *Cribroperidinium* are common components of the dinoflagellate cyst assemblages from sub-palynofacies B2.

over mudstone levels and symmetrically straight to sinuous ripples as bedforms, wave truncation structure and isotropic HCS. Carbonaceous remains are often found, dispersed or overlying boundary surfaces, with mica fragments along laminae. Disarticulated, fragmented valves and dispersed gastropods are often found. Sandstone beds show traces of *Arenicolites*, *Gyrochorte* and *Skolithos* (Fig. 4f).

Facies HeL is made up of massive to laminated black mudstones with well-sorted massive to diffuse laminated sandstone intercalations (the latter with a

variable thickness between 3 and 10 cm). Sandstones represent less than 15% of the facies and it is very common to find symmetrical ripples with wave truncation structure (lenticular bedding). Dispersed plant remains are found also associated with micas overlying boundary surfaces. Small bivalves (articulated, disarticulated and fragmented) and dispersed gastropods (up to 5 mm) are common. Thicker levels of sand may have erosive bases.

These heterolithic facies usually conform thickening and coarsening-upward cycles, from lenticular

to flaser heterolithic, which then grade into more sandy facies.

Interpretation: Reineck and Wunderlich (1968) defined heterolithic deposits as a regular centimeter alternation between fine sandstones (with different sedimentary structures) and mudstones (massive or laminated). These facies would be formed from the alternation of fallout and traction-plus-fallout processes from long-lived waxing (sand transport by suspended load and wave-enhanced suspension) and waning flows (low energy conditions and deposition of clay and silt by normal settling) (Bhattacharya and MacEachern, 2009; Ponce *et al.*, 2015).

The *Arenicolites* and *Skolithos* traces recognized in HeW facies, are developed by suspension feeding organism and occur in periods with high energy and suspended load (Buatois and Mángano, 2011), whereas Gyrochorte traces are developed by deposit-feeding organisms that colonize the substrate during low to moderate energy and benthic food availability periods (Buatois and Mángano, 2011; Wetzel *et al.*, 2020).

4.1.3. Muddy facies (FM, FL and FLc)

FM facies is made up of massive black to greyish clayey silt and sandy silt. In general, this facies is deposited over sharp basal boundaries on sandy or calcareous facies and transitionally grades up into lenticular/wavy heterolithic or massive/laminated sandy facies. It may contain dispersed carbonaceous remains.

FL facies is composed of laminated black to greyish clayey silt and sandy silt, which may have small disarticulated (and in some cases also fragmented) valves between sheets. Carbonaceous remains are often found between laminae. In general, they are in sharp contact over psammitic deposits and grade up into heterolithic to massive/laminated sand facies composing thickening- and coarsening-upward cycles (Fig. 4e).

Finally, FLc facies corresponds to laminated calcareous mudstones, often showing gastropods between laminae.

Eight samples were analyzed, in these facies, for palynological organic matter in the Bajada del Agrio Section. From this analysis two palynofacies could be recognized (Fig. 5). Palynofacies A exhibits a predominance of terrestrial-derived components, mainly phytoclasts with proportions greater than 80%, marine-derived amorphous organic matter (AOM) lower than 2.8%, and palynomorphs reach up to 11.6%. The ratio of terrestrial (pollen and spores) to marine palynomorphs (dinoflagellate cysts) (T/M) varies between 2.5% and 13%. Palynofacies B shows proportions of phytoclasts between 57% and 78%, AOM lower than 3.2% and

palynomorphs between 21% and 43%. In turn, the latter can be subdivided in two sub-palynofacies: sub-palynofacies B1, with dinoflagellate cysts between 9% and 13% and approximately T/M between 1% and 3%, and sub-palynofacies B2 with higher proportions of dinoflagellate cysts (22%–26%) and a T/M lower than 0.5%.

Interpretation: The deposition of clay–silt in marine environments has historically been associated with the fallout of suspended fine-grained materials from calm waters in offshore environments (Pettijohn, 1975; Bhattacharya and Walker, 1992; Nichols, 1999; Potter *et al.*, 2005). However, recent studies have shown that fine-grained sediments can be deposited by mud-rich flows under more energetic conditions (Schieber and Yawar, 2009). These flows can transport clay–silt particles for long distances as bed load and suspended load (Otharín, 2020; Otharín *et al.*, 2020). The transport and deposition of flocculated mud in currents occur with flow speeds that can also transport and accumulate sands (Schieber *et al.*, 2007). In fact, many modern shelf muds are recognized as accumulating in prodelta settings related to hyperpycnal mud plumes generated in coastal areas during river floods (Bhattacharya and MacEachern, 2009).

In their experiments, Schieber *et al.* (2007) demonstrated that some clay beds formed downcurrent-inclined laminae (low-angle ripples). Once fully compacted, these low-angle ripples often appear as parallel-laminated mudstones. Therefore, facies FL may have an alternative origin related to migrating floccule ripples (Schieber *et al.*, 2007; Schieber and Southard, 2009; Schieber and Yawar, 2009). Regarding facies FM, the distinction between massive mudstones accumulated in prodelta or shelfal settings can be very difficult (Zavala and Pan, 2018).

The dinoflagellate cyst species identified in the samples are those expected for the late Hauterivian of the Neuquén Basin, having been previously recognized in other sections of the Agrio Formation (Guler *et al.*, 2016; Paolillo *et al.*, 2018; Omarini *et al.*, 2020). The high proportions of phytoclasts and sporomorphs indicate an important terrestrial input, while the presence of dinoflagellate cysts in all samples (between 0.2% and 26%) denotes the marine origin of the sediments.

4.1.4. Calcareous facies (Cm, Cw, Cp and Cg facies)

Calcareous facies are commonly found at the top of progradational clastic facies successions. These carbonates were classified according to Dunham (1962). Four calcareous facies were recognized, termed facies Cm, Cw, Cp and Cg. In general, these facies show an orange coloration on the outside and greyish inside.

The Cm facies is a mudstone (mud-supported calcareous rock) with a few remains of fragmented valves.

The Cw facies is a wackestone (mud-supported calcareous rock), with floating articulated, disarticulated and fragmented valves without a dominant orientation. Serpulids are also common in bioclasts valves, and in replaced gastropods and ammonoids. These rocks are arranged in a tabular way in sharp contact over mudstone or sandstone deposits.

Cp facies is a packstone (bioclastic grain-supported calcareous rock) with articulated, disarticulated and fragmented valve remains, disposed of without orientation. External and internal valves are observed. They are arranged in sharp contact over muddy or sandy facies (Fig. 4g). This facies is characterized by having articulated bivalves of up to 40 cm in El Mojado and Bajada del Agrio sections.

The Cg facies is made up of grainstone (grain-supported calcareous rock) without matrix, with isolated articulated (4–5 cm), disarticulated and fragmented valves.

Interpretation: The most used classifications for carbonates are those based on the concept of textural maturity since it is believed that it is related to the energy level during the deposition of limestones (Tucker and Wright, 1990). The simplest and most widely used classification is that of Dunham (1962). However, the wide spectrum of mixed sediments that exist between siliciclastic and carbonate rocks has been largely ignored (Mount, 1985). Some authors like Folk (1962, 1974), Pettijohn (1975) and Zuffa (1980) had described mixed (siliciclastic–carbonate) sediments, although these classifications are of difficult application for the systematic description of the complete range between siliciclastic and carbonate rocks. Mount (1985) proposed a descriptive classification for these rocks based on a series of questions about the composition and texture of the samples.

4.2. Facies associations

4.2.1. Offshore/prodelta facies association (FM, FL, Cw, Cp, SfM)

This facies association is mainly composed of massive and laminated mudstone facies. They are arranged with a tabular geometry and deposited over sharp bases with a thickness up to 65 m. Mudstone deposits are intercalated with calcareous facies up to 2.5 m thick and massive sandstone levels of up to 30 cm thick with calcareous concretions and valve remains.

In some cases, mudstone facies are poorly exposed. Undifferentiated bioturbation is recognized in these facies. This facies association is common near the base of the Bajada del Agrio profile.

The offshore/prodelta facies association corresponds to sediments deposited below the fair-weather wave base where, in general, calm water conditions are dominant. Thin sandy levels could represent small and isolated storm events or deposits related to weak turbulent flows.

4.2.2. Distal ramp delta facies association (FM, FL, FLc, Cw, Cp, Cg, HeL, HeW, SfM)

The distal ramp delta facies association (DRD) is composed of tabular bodies of massive and laminated mudstone lying on sharp bases. Carbonaceous remains and fragmented valves are common between laminae, often interbedded with calcareous facies. Lenticular and wavy heterolithic facies are also part of this association, transitionally grading from mudstone facies and reaching a thickness up to 55 m. Heterolithic facies can also be observed at the base of thickening- and coarsening-upward cycles.

In this association, some prodelta lobes made up of massive sands can be distinguished in sharp contact over mudstone facies with thicknesses ranging from a few centimeters up to 2 m approximately.

The distal ramp delta facies association is located at the distal part of a low gradient littoral delta system. The presence of carbonaceous remains would indicate a connection with an active fluvial discharge. Calcareous facies intercalations on tops could indicate a pause in the sediment supply and in the resulting prograding system. Development of traction-plus-fallout processes is observed, characterized by heterolithic facies.

4.2.3. Proximal ramp delta facies association (SfM-SfL-SfW-SfR-SfH-SfX-Hef)

The proximal ramp delta facies association (PRD) shows a tabular geometry. In general, they are arranged in a transitional way over mudstone or heterolithic facies (from the DRD), forming thickening- and coarsening-upward cycles. Sandy facies can also be found in sharp contact over mudstone facies, forming tabular bodies up to 6 m thick. Frequently, sandy levels (less than 2 m thick) are observed with sandy facies in transitional contact between them.

This association represents the main sandy section of a low-gradient deltaic system, with sedimentary structures that would indicate traction-plus-fallout

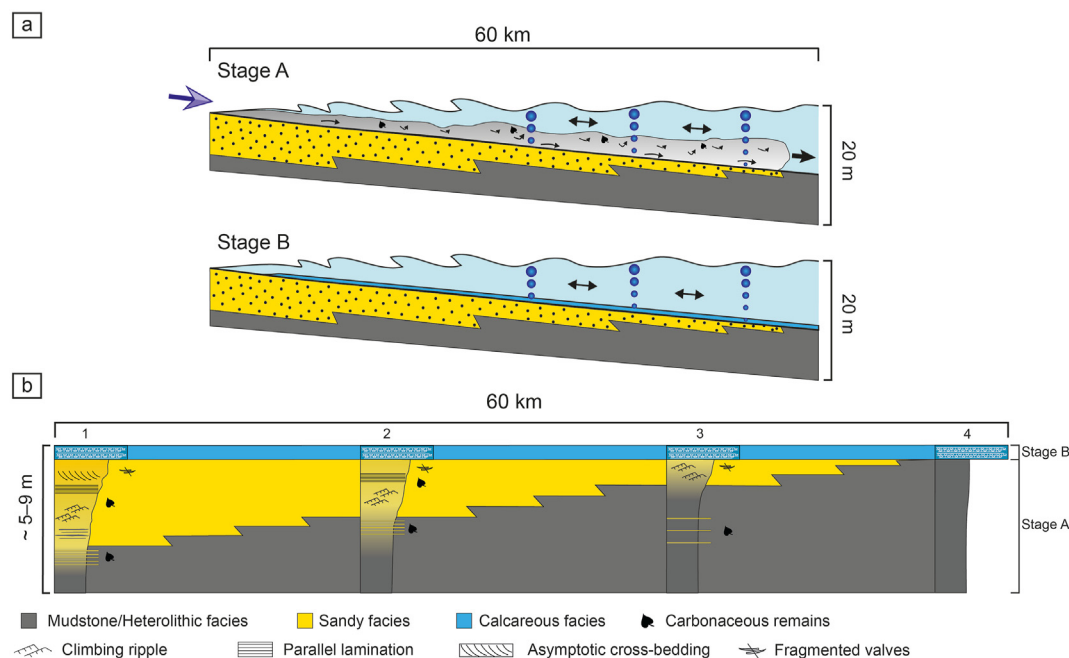


Fig. 6 Internal stacking patterns observed in EDS. **a** Diagram showing the proposed origin of EDS, related to the supply of turbulent suspensions from the continent (Stage A) by hyperpycnal flows, forming a long-gradient delta front deposit (HLD). The suspended sediments can be maintained in the flow for long distances aided by wave action (Zavala et al., 2021). During Stage B, the sediment supply ceased, and the “normal” marine conditions were reestablished in the host basin (with the precipitation of carbonates and development of benthic life). **b** Schema showing facies changes along prograding EDS sequences, showing a gradual transition from shales to sandy facies, culminating in bioclastic calcareous levels. These EDS often range between 5 and 9 m thick approximately. 1, 2, 3 and 4: The four schematic sections, which are the same ones as shown in Fig. 7.

processes in channels and unconfined sediment-laden turbulent flows. The abundant presence of carbonaceous remains would indicate a direct supply from an active fluvial discharge.

The low-to-moderate abundance and diversity of trace fossils indicate stressed environments related to brackish-water influence, high water turbidity and high sedimentation rate (Buatois and Mángano, 2011). The presence of trace fossils developed by deposit-feeding organism (*Gyrochorte*, *Hillichnus*, *Lockeia* and *Sinusichnus*) in marine sandstones deposited under high-to-moderate energy, indicates high turbidity in waters that inhibit the occurrence of suspension-feeding organism (MacEachern et al., 2005). The presence of fossil traces originated by suspension-feeding organism (*Arenicolites*, *Ophiomorpha* and *Skolithos*) associated to the top of sandstones beds, evidences the occurrence of opportunistic organism that colonized the substrate between periods of bars construction (Buatois and Mángano, 2011). The occurrence of scape traces can be related to high aggradational rates produced by hyperpycnal flow (Buatois and Mángano, 2011).

5. Discussion

The Agua de la Mula Member was previously interpreted as accumulating in a basinal to inner homoclinal ramp system with storm influence (Spalletti et al., 2001a, 2001b; Lazo et al., 2005; Sagasti, 2005). Towards the upper part of the unit, the increasing influence of waves and tides has been previously mentioned by several authors (Tunik et al., 2009; Fernández and Pazos, 2012; Pazos et al., 2012). The stratigraphic sections located at the southeast in the studied area are considered to be accumulated in a mid-ramp to inner ramp setting, while to the north, outer-ramp to distal mid-ramp deltaic conditions would develop (Spalletti et al., 2001a, 2001b; Fernández and Pazos, 2012; Guler et al., 2013; Comerio, 2016; Fernández et al., 2019).

A correlation panel (Fig. 2) allowed us to recognize the main geometry of the sedimentary bodies and their stacking pattern, which corresponds to a low gradient delta system composed of several shallowing-upward and prograding elementary depositional sequences

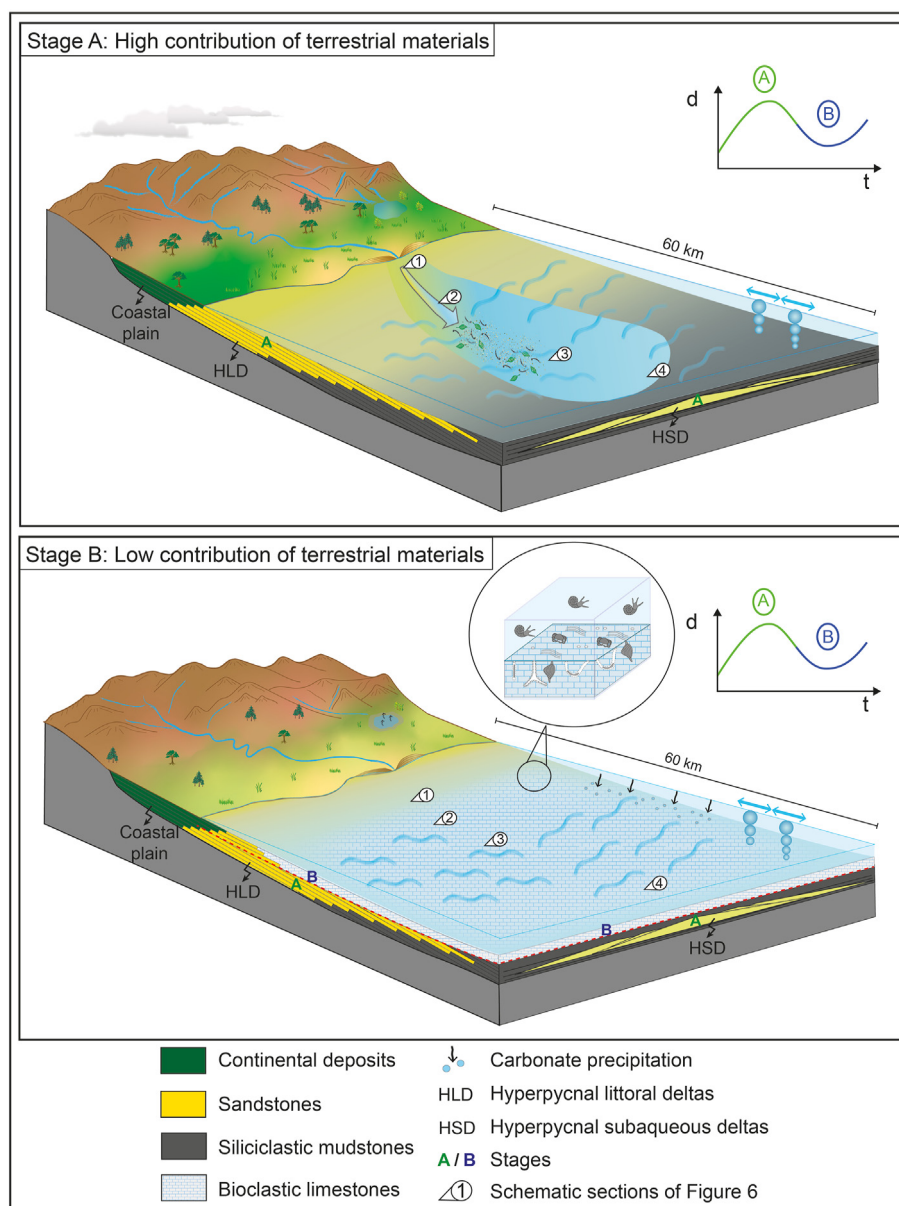


Fig. 7 Depositional model of hyperpycnal littoral deltas (HLD) in the Agua de la Mula Member. **a** During Stage A, the cyclic contribution of clastic materials during humid climatic conditions by sediment-laden fluvial discharges (weak hyperpycnal flows) results in the progradation of sandy facies on offshore/prodelta facies associations. The long distance is explained by the low gradient. **b** During Stage B, there is a cessation in the clastic supply from the continent, with a reestablishment of the normal marine salinity conditions and related precipitation of carbonates.

(EDS, in the sense of Mutti *et al.*, 1994a). These EDS show a gradual transition between fine-grained offshore deposits and shallow water sandy facies, showing an increased influence of wave action towards the top. Internally, the EDS show a coarsening- and thickening-upward trend, accompanied by an increasing content in particulate organic matter and micas. These deposits are characterized by a moderate to low ichnodiversity and abundance. In general, these prograding EDS culminate with massive sandstones with bioclasts,

followed in sharp contact by bioclastic limestones (Fig. 6). This upper interval probably suggests a cessation of the clastic supply from the continent, with a reestablishment of marine salinity, which favours the precipitation of carbonates. These prograding cycles could be linked to allocyclic processes (Beerbower, 1964) characterized by the cyclic contribution of clastic material during humid climatic conditions by sediment-laden fluvial discharges (Fig. 7a) accumulated in low-gradient (ramp) deltas, alternating with periods

of low sediment supply, and the accumulation of carbonate levels (Fig. 7b). Field evidence shows that these shallowing-upward and prograding cycles are developed within a totally marine context. These shallowing-upward —progradational EDS can be traced for 100's of kilometers without showing equivalent delta plain facies in the study area.

Littoral delta systems developed under normal marine salinity conditions have been classified taking into account the density contrast between the incoming and host water, the size of the sediment and the importance of fluvial, waves and tidal processes at coastal areas (Bates, 1953; Galloway, 1975). However, deltas can be very diverse and escape conventional classifications, as is the case of the Volga delta of the Caspian Sea, considered a fluvial-dominated delta (according to Galloway, 1975) and type 8 (according to the Postma, 1995 classification). This delta is characterized by a very low gradient delta front, forming a ramp delta (Overeem *et al.*, 2003). These ramp deltas are also often called “prodelta hyperpynites” (Zavala *et al.*, 2006, 2011; Bhattacharya and MacEachern, 2009; Wilson and Schieber, 2014) or “wave enhanced turbulent flows” (Wilson and Schieber, 2014), where the effect of waves can aid hyperpynal flows to travel many kilometers into the basin generating very-low-gradient delta fronts. For Wilson and Schieber (2014) the deposits produced by these flows are composed of graded intervals of shales and sands. These deposits show variations of internal sedimentary structures that suggest fluctuations in quasi-steady flows. Ramp deltas have slopes of less than 1° , with delta fronts that can extend for hundreds of kilometers with little changes in facies and grain size. Their associated deposits show abundant plant remains and display different orders of cyclicity, where the highest order is composed of coarsening- and thickening-upward cycles in all, similar to the parasequences proposed for eustatic cycles (Van Wagoner *et al.*, 1990). In a recent contribution, Zavala *et al.* (2021) proposed a new classification for deltaic deposits considering the relationship between the density of incoming flows and the salinity of the receiving water body. Within these new deltaic categories, ramp deltas were termed hyperpynal littoral deltas (HLD). These HLD form when weak sustained hyperpynal flows enter in marine or brackish basins. Due to their relatively low density, these hyperpynal flows do not produce a substantial erosion of the sea bottom (for example eroding channels). In contrast, sediments in these diluted plumes can be maintained in suspension for long distances aided by wave action along very low As a summary, it is interpreted that the Agua de la Mula Member was accumulated by stacked hyperpynal littoral deltas.

Regional data suggest for the studied interval a depositional slope of 0.02° , which is consistent with the proposed slopes for HLD's (Zavala *et al.*, 2021). The volume of freshwater introduced to this shallow shelf during delta progradation probably contributed to reducing the overall salinity of the basin resulting in brackish conditions. These brackish conditions are also evidenced by the low to moderate diversity and abundance of trace fossil, with a predominance of biogenic structures generated by detritivorous organisms over those generated by suspensivorous organisms. The basinward progradation of these low-gradient delta front deposits generated by weak hyperpynal discharges results in coarsening- and thickening-upward cycles, with abundant content of micaceous and bioclasts. The high proportions of phyto-clasts (between 57% and 80%) among the organic matter suggest an important terrestrial influx within the marine basin. These progradational cycles culminate with fossiliferous calcareous levels that indicate a cessation of continental input and probably a return to normal salinity conditions. The presence of stacking sets of progradational cycles allows to infer the occurrence of successive activations of hyperpynal littoral deltas (HLD). These deltaic deposits can be regionally recognized in the study area extended for tens of kilometers without developing coeval delta plain (continental) deposits. During exceptional river discharges, the incoming flow can eventually bypass the coastal area, accumulating hyperpynal subaqueous deltas (HSD) composed of channels and lobes at inner basin areas (Fig. 7; Zavala *et al.*, 2021).

6. Conclusions

In the study region, the Agua de la Mula Member is characterized by a progradational succession composed of stacked m-thick very low gradient ramp delta deposits, originated by sustained low-density hyperpynal flows, corresponding to hyperpynal littoral deltas (HLD). These HLD extend for tens to hundreds of kilometers in shallow areas of the basin, with clastic deposits distributed by diluted hyperpynal flows aided by wave action. During delta progradation, the increasing input of freshwater could generate brackish conditions, specially in shallow waters, which is evidenced by the virtual absence of body fossils and the low to moderate bioturbation of these deposits. On the contrary, when water and sediment supply decreased, the salinity of the sea water gradually increased, favoring the colonization of the sea bottom by benthic organisms, and therefore the

development of bioclastic mixed limestones (condensed intervals) on top of progradational sequences. Body fossils in these bioclastic intervals appear highly-disturbed by wave action, evidencing shallow water conditions periodically affected by wave action. The apparent marine transgression observed on top of these small-scale sequences, characterized by offshore shales lying over a sharp boundary is probably related to the combined effect of low sediment supply and regional subsidence, resulting in a relative sea level rise.

Small-scale progradational sequences are in turn stacked composing different low-order sequences that can be traced at a basinward scale. At inner basin areas, preliminary data suggest that distal HLD alternate with hyperpycnal subaqueous delta (HSD) deposits. The interaction between these two delta types in the Agua de la Mula Member is still poorly understood and will require additional studies.

Abbreviations

AOM	Amorphous organic matter
BA	Bajada del Agrio section
Cg	Grainstone calcareous facies
Cm	Mudstone calcareous facies
Cp	Packstone calcareous facies
Cw	Wackestone calcareous facies
DRD	Distal ramp delta facies association
EDS	depositional sequences
EM	El Mojado section
FL	Laminated muddy facies
FLc	Laminated calcareous muddy facies
FM	Massive muddy facies
HCS	Hummocky cross-stratification
HeF	Flaser heterolithic facies
HeL	Lenticular heterolithic facies
HeW	Wavy heterolithic facies
HLD	Hyperpycnal littoral deltas
HSD	Hyperpycnal subaqueous deltas
LQ	La Quebrada section
PRD	Proximal ramp delta facies association
SfH	Hummocky sandy facies
SfHa	Anisotropic hummocky sandy facies
SfHi	Isotropic hummocky sandy facies
SfL	Laminated fine-grained sandy facies
SfM	Massive fine-grained sandy facies
SfR	Climbing ripple fine-grained sandy facies
SfW	Wave truncated sandy facies
SfX	Asymptotic and trough cross-bedding sandy facies

T/M Terrestrial versus marine palynomorphs

Availability of data and materials

All data generated or analyzed during this study are included in this published article.

Funding

The present work was financed by CONICET PUE0047CO and ANPCyT 0419 projects.

Competing interests

The authors declare that they have no competing interests.

Authors' contributions

AI and CZ actively discussed the main idea, designed figures and wrote the manuscript. DMC provided trace fossils information, helped and designed some figures and participated in facies analysis and depositional model discussion. MT, FP, DO and MI provided fundamental support during field work and actively participated in discussing deltaic sedimentation. PM analyzed palynological samples.

Acknowledgements

We appreciate logistical support of the Geology Department of the Universidad Nacional del Sur. We kindly acknowledge the people from Bajada del Agrio and Las Lajas localities for their hospitality, and Natalia Sánchez, Gaspar Peñalva and Trinidad Duran for their field discussion and collaboration.

References

- Aguirre-Urreta, B., Schmitz, M., Lescano, M., Tunik, M., Rawson, P.F., Concheyro, A., Buhler, M., Ramos, V.A., 2017. A high precision U-Pb radioisotopic age for the Agrio Formation, Neuquén Basin, Argentina: implications

- for the chronology of the Hauterivian Stage. *Cretaceous Research*, 75, 193–204. <https://doi.org/10.1016/j.cretres.2017.03.027>.
- Aguirre-Urreta, B., Martinez, M., Schmitz, M., Lescano, M., Omarini, J., Tunik, M., Kuhnert, H., Concheyro, A., Rawson, P.F., Ramos, V.A., Reboulet, S., Noclin, N., Frederichs, T., Nickl, A.L., Pálke, H., 2019. Interhemispheric radio-astrochronological calibration of the time scales from the Andean and the Tethyan areas in the Valanginian–Hauterivian (Early Cretaceous). *Gondwana Research*, 70, 104–132. <https://doi.org/10.1016/j.gr.2019.01.006>.
- Aguirre-Urreta, M.B., Rawson, P.F., 1997. The ammonite sequence in the Agrio Formation (Lower Cretaceous), Neuquén Basin, Argentina. *Geological Magazine*, 134(4), 449–458. <https://doi.org/10.1017/S0016756897007206>.
- Allen, J.R.L., 1984. Parallel lamination developed from upper-stage plane beds: A model based on the larger coherent structures of the turbulent boundary layer. *Sedimentary Geology*, 39(3–4), 227–242. [https://doi.org/10.1016/0037-0738\(84\)90052-6](https://doi.org/10.1016/0037-0738(84)90052-6).
- Allen, P.A., Pound, C.J., 1985. Storm sedimentation. *Journal of the Geological Society*, 142(2), 411–412. <https://doi.org/10.1144/gsjgs.142.2.0411>.
- Arnott, R.W.C., Hand, B.M., 1989. Bedforms, primary structures and grain fabric in the presence of suspended sediment rain. *Journal of Sedimentary Petrology*, 59(6), 1062–1069. <https://doi.org/10.1306/212F90F2-2B24-11D7-8648000102C1865D>.
- Arnott, R.W., Southard, J.B., 1990. Exploratory flow-duct experiments on combined-flow bed configurations, and some implications for interpreting storm-event stratification. *Journal of Sedimentary Petrology*, 60(2), 211–219. <https://doi.org/10.1306/212F9156-2B24-11D7-8648000102C1865D>.
- Arregui, C., Carbone, O., Leanza, H.A., 2011. Contexto tectosedimentario. In: Leanza, H.A., Arregui, C., Carbone, O., Danieli, J.C., Vallés, J.M. (Eds.), *Relatorio del XVIII Congreso Geológico Argentino. Geología y Recursos Naturales de la provincia de Neuquén. Asociación Geológica Argentina*, pp. 29–36.
- Ashley, G.M., Southard, J.B., Boothroyd, J.C., 1982. Deposition of climbing-ripple beds: A flume simulation. *Sedimentology*, 29(1), 67–79. <https://doi.org/10.1111/j.1365-3091.1982.tb01709.x>.
- Banerjee, I., 1977. Experimental study on the effect of deceleration on the vertical sequence of sedimentary structures in silty sediments. *Journal of Sedimentary Petrology*, 47(2), 771–783. <https://doi.org/10.1306/212F7248-2B24-11D7-8648000102C1865D>.
- Barron, E.J., 1989. Severe storms during Earth history. *GSA Bulletin*, 101(5), 601–612. [https://doi.org/10.1130/0016-7606\(1989\)101<0601:SSDEH>2.3.CO;2](https://doi.org/10.1130/0016-7606(1989)101<0601:SSDEH>2.3.CO;2).
- Bates, C.C., 1953. Rational theory of delta formation. *AAPG Bulletin*, 37(9), 2119–2162. <https://doi.org/10.1306/5CEADD76-16BB-11D7-8645000102C1865D>.
- Beerbower, J.R., 1964. Cyclothems and cyclic depositional mechanisms in alluvial plain sedimentation. *Kansas State Geological Survey, Bulletin*, 169, 31–42.
- Bhattacharya, J.P., 2006. Deltas. In: Posamentier, H.W., Walker, R.G. (Eds.), *Facies Models Revisited*. SEPM Special Publication, vol. 84, pp. 237–292. <https://doi.org/10.2110/pec.06.84.0237>.
- Bhattacharya, J.P., MacEachern, J.A., 2009. Hyperpynal rivers and prodeltaic shelves in the Cretaceous seaway of North America. *Journal of Sedimentary Research*, 79(4), 184–209. <https://doi.org/10.2110/jsr.2009.026>.
- Bhattacharya, J.P., Walker, R.G., 1992. Deltas. In: Walker, R.G., James, N.P. (Eds.), *Facies Models: Response to Sea Level Change*. Geological Association of Canada, pp. 157–177.
- Bromley, R.G., Uchman, A., Gregory, M.R., Martin, A.J., 2003. *Hillichnus lobosensis* igen. et isp. nov., a complex trace fossil produced by tellinacean bivalves, Paleocene, Monterey, California, USA. *Palaeogeography, Palaeoclimatology, Palaeoecology*, 192, 157–186. [https://doi.org/10.1016/S0031-0182\(02\)00684-3](https://doi.org/10.1016/S0031-0182(02)00684-3).
- Buatois, L.A., Mángano, M.G., 2011. *Ichnology, Organism-Substrate Interactions in Space and Time*. Cambridge University Press, Cambridge.
- Burgess, P.M., Flint, S., Johnson, S., 2000. Sequence stratigraphic interpretation of turbiditic strata: An example from Jurassic strata of the Neuquén Basin, Argentina. *GSA Bulletin*, 112(11), 1650–1666. [https://doi.org/10.1130/0016-7606\(2000\)112<1650:SSIOTS>2.0.CO;2](https://doi.org/10.1130/0016-7606(2000)112<1650:SSIOTS>2.0.CO;2).
- Camacho, H., Busby, C.J., Kneller, B., 2002. A new depositional model for the classical turbidite locality at San Clemente State Beach, California. *AAPG Bulletin*, 86(9), 1543–1560. <https://doi.org/10.1306/61EEDCF6-173E-11D7-8645000102C1865D>.
- Campbell, C.V., 1966. Truncated wave-ripple laminae. *Journal of Sedimentary Petrology*, 36(3), 825–828.
- Carmona, N.B., 2005. *ICNología del Mioceno marino en la región del golfo San Jorge*. PhD thesis. Departamento de Ciencias Geológicas, Facultad de Ciencias Exactas y Naturales, Universidad de Buenos Aires.
- Comerio, M., 2016. *Estudio mineralógico de las arcillas del Miembro Agua de la Mula –Formación Agrio, en un marco estratigráfico secuencial, en el Engolfamiento Neuquino*. PhD thesis. Universidad de Buenos Aires.
- Comerio, M., Fernández, D.E., Gutiérrez, C., Ballivián Justiniano, C., González Estebenet, M.C., Pazos, P.J., 2019. Sedimentary evolution of the marine Agua de la Mula member (Agrio Formation, Lower Cretaceous) in the central Neuquén Basin: Source areas and paleogeographic considerations from a distal setting. *Journal of South American Earth Sciences*, 96, 102259. <https://doi.org/10.1016/j.jsames.2019.102259>.
- Comerio, M., Fernández, D.E., Pazos, P.J., 2018. Sedimentological and ichnological characterization of muddy storm related deposits: The upper Hauterivian ramp of the Agrio Formation in the Neuquén Basin, Argentina. *Cretaceous Research*, 85, 78–94. <https://doi.org/10.1016/j.cretres.2017.11.024>.
- Dott Jr., R.H., Bourgeois, J., 1982. Hummocky stratification: Significance of its variable bedding sequences. *GSA Bulletin*, 93(8), 663–680. [https://doi.org/10.1130/0016-7606\(1982\)93<663:HSSOIV>2.0.CO;2](https://doi.org/10.1130/0016-7606(1982)93<663:HSSOIV>2.0.CO;2).
- Dott Jr., R.H., Bourgeois, J., 1983. Hummocky stratification: Significance of its variable bedding sequences: Discussion and reply: Reply. *Geological Society of America Bulletin*,

- 94(10), 1249–1251. [https://doi.org/10.1130/0016-7606\(1983\)94<1249:HSSOIV>2.0.CO;2](https://doi.org/10.1130/0016-7606(1983)94<1249:HSSOIV>2.0.CO;2).
- Dumas, S., Arnott, R.W.C., 2006. Origin of hummocky and swaley cross-stratification — The controlling influence of unidirectional current strength and aggradation rate. *Geology*, 34(12), 1073–1076. <https://doi.org/10.1130/G22930A.1>.
- Dumas, S., Arnott, R.W.C., Southard, J.B., 2005. Experiments on oscillatory-flow and combined-flow bed forms: Implications for interpreting parts of the shallow-marine sedimentary record. *Journal of Sedimentary Research*, 75(3), 501–513. <https://doi.org/10.2110/jsr.2005.039>.
- Dunham, R.J., 1962. Classification of carbonate rocks according to depositional texture. In: Ham, W.E. (Ed.), *Classification of Carbonate Rocks*. AAPG Memoir, vol. 1, pp. 108–121.
- Fernández, D.E., Comerio, M., Giachetti, L.M., Pazos, P.J., Wetzel, A., 2019. Asteroid trace fossils from Lower Cretaceous shallow- to marginal-marine deposits in Patagonia. *Cretaceous Research*, 93, 120–128. <https://doi.org/10.1016/j.cretres.2018.09.010>.
- Fernández, D.E., Pazos, P.J., 2012. Ichnology of marginal marine facies of the Agrio Formation (Lower Cretaceous, Neuquén Basin, Argentina) at its type locality. *Ameghiniana*, 49(4), 505–524.
- Folk, R.L., 1962. Spectral subdivision of limestone types. In: Ham, W.E. (Ed.), *Classification of Carbonate Rocks — A Symposium*, vol. 1. AAPG Memoir, pp. 62–84.
- Folk, R.L., 1974. *Petrology of Sedimentary Rocks*, 2nd ed. Hemphill Publishing Company, Austin, Texas.
- Franzese, J.R., Spalletti, L.A., 2001. Late Triassic–Early Jurassic continental extension in southwestern Gondwana: Tectonic segmentation and pre-break-up rifting. *Journal of South American Earth Sciences*, 14(3), 257–270. [https://doi.org/10.1016/S0895-9811\(01\)00029-3](https://doi.org/10.1016/S0895-9811(01)00029-3).
- Galloway, W.E., 1975. Process framework for describing the morphologic and stratigraphic evolution of deltaic depositional systems. In: Broussard, M.L. (Ed.), *Deltas: Models for Exploration*. Houston Geological Society, Houston, pp. 87–98.
- Guler, M.V., Lazo, D.G., Pazos, P.J., Borel, C.M., Ottone, E.G., Tyson, R.V., Cesaretti, N., Aguirre-Urreta, M.B., 2013. Palynofacies analysis and palynology of the Agua de la Mula member (Agrio Formation) in a sequence stratigraphy framework, Lower Cretaceous, Neuquén Basin, Argentina. *Cretaceous Research*, 41, 65–81. <https://doi.org/10.1016/j.cretres.2012.10.006>.
- Guler, M.V., Paolillo, M.A., Martz, P.A., 2016. Early Cretaceous dinoflagellate cysts from the Neuquén and Austral basins: A review. *Asociación paleontológica Argentina. Physician Executive*, 16(2), 76–87.
- Gulisano, C.A., 1981. El ciclo cuyano en el norte de Neuquén y sur de Mendoza. San Luis. In: 8° Congreso Geológico Argentino, vol. 3, pp. 573–592.
- Gulisano, C.A., Gutiérrez Pleimling, A.R., 1988. Depósitos eólicos del Miembro Avilé (Formación Agrio, Cretácico Inferior) en el norte del Neuquén, Argentina. Buenos Aires. *Reproduction. Abstract Series* 120–124. Proceeding.
- Gulisano, C.A., Gutiérrez Pleimling, A.R., 1995. *Field Guide: The Jurassic of the Neuquén Basin, a) Neuquén Province. Buenos Aires*. Asociación Geológica Argentina, Serie D.
- Harms, J.C., 1969. Hydraulic significance of some sand ripples. *GSA Bulletin*, 80(3), 363–396. [https://doi.org/10.1130/0016-7606\(1969\)80\[363:HSSSRJ\]2.0.CO;2](https://doi.org/10.1130/0016-7606(1969)80[363:HSSSRJ]2.0.CO;2).
- Harms, J.C., Southard, J.B., Spearing, D.R., Walker, R.G., 1975. Depositional environments as interpreted from primary sedimentary structures and stratification sequences. *SEPM Short Course Notes*, 2, 1–161. <https://doi.org/10.2110/scn.75.02>.
- Harms, J.C., Southard, J.B., Walker, R.G., 1982. Structures and sequences in clastic rocks. *SEPM Short Course Notes*, 9, 1–249. <https://doi.org/10.2110/scn.82.09>.
- Howell, J.A., Schwarz, E., Spalletti, L.A., Veiga, G.D., 2005. The Neuquén Basin: An overview. In: Veiga, G.D., Spalletti, L.A., Howell, J.A., Schwarz, E. (Eds.), *The Neuquén Basin, Argentina: A Case Study in Sequence Stratigraphy and Basin Dynamics*, vol. 252. Geological Society, London, Special Publications, pp. 1–14. <https://doi.org/10.1144/GSL.SP.2005.252.01.01>.
- Irastorza, A., Turienzo, M., Peralta, F., Irastorza, M., Zavala, C., Sánchez, N., 2019. La estructura del frente de deformación de la faja plegada y corrida del Agrio a los 38°20'S, Cuenca Neuquina. *Revista de la Asociación Geológica Argentina*, 76(3), 213–228.
- Jopling, A.V., Walker, R.G., 1968. Morphology and origin of ripple-drift cross-lamination, with examples from the Pleistocene of Massachusetts. *Journal of Sedimentary Petrology*, 38(4), 971–984. <https://doi.org/10.1306/74D71ADC-2B21-11D7-8648000102C1865D>.
- Kietzmann, D.A., Folguera, A., 2020. *Opening and Closure of the Neuquén Basin in the Southern Andes*. Springer Earth System Sciences.
- Kneller, B.C., Branney, M.J., 1995. Sustained high-density turbidity currents and the deposition of thick massive sands. *Sedimentology*, 42(4), 607–616. <https://doi.org/10.1111/j.1365-3091.1995.tb00395.x>.
- Lazo, D.G., Cichowolski, M., Rodríguez, D.L., Aguirre-Urreta, M.B., 2005. Lithofacies, palaeoecology and palaeoenvironments of the Agrio Formation, Lower Cretaceous of the Neuquén Basin, Argentina. In: Veiga, G.D., Spalletti, L.A., Howell, J.A., Schwarz, E. (Eds.), *The Neuquén Basin, Argentina: A Case Study in Sequence Stratigraphy and Basin Dynamics*. Geological Society, London, Special Publications, vol. 252, pp. 295–315. <https://doi.org/10.1144/GSL.SP.2005.252.01.15>.
- Leanza, H.A., Hugo, C.A., Repol, D., Gonzalez, R., Danieli, J.C., 2001. *Hoja Geológica 3969-I Zapala, Provincia del Neuquén*. Buenos Aires: Servicio Geológico Minero Argentino, Instituto de Geología y Recursos Minerales, Boletín, vol. 275.
- Legarreta, L., Uliana, M.A., 1991. Jurassic–Cretaceous marine oscillations and geometry of back-arc basin fill, central Argentine Andes. In: McDonald, D.I.M. (Ed.), *Sedimentation, Tectonics and Eustasy*. IAS Special Publication, vol. 12, pp. 429–450.
- Legarreta, L., Uliana, M.A., 1999. El jurásico y cretácico de la Cordillera principal y la Cuenca neuquina. In: Caminos, R. (Ed.), *En Geología Argentina*. Buenos Aires:

- Servicio Geológico Minero Argentino, *Anales*, vol. 29, pp. 399–416.
- López Cabrera, M.I., Mángano, M.G., Buatois, L.A., Olivero, E.B., Maples, C.G., 2019. Bivalves on the move: The interplay of extrinsic and intrinsic factors on the morphology of the trace fossil *Protovirgularia*. *Palaios*, 34(7), 349–363. <https://doi.org/10.2110/palo.2019.004>.
- Macdonald, D., Gomez-Perez, I., Franzese, J., Spalletti, L., Lawver, L., Gahagan, L., Dalziel, I., Thomas, C., Trewin, N., Hole, M., Paton, D., 2003. Mesozoic break-up of SW Gondwana: Implications for regional hydrocarbon potential of the southern South Atlantic. *Marine and Petroleum Geology*, 20(3–4), 287–308. [https://doi.org/10.1016/S0264-8172\(03\)00045-X](https://doi.org/10.1016/S0264-8172(03)00045-X).
- MacEachern, J.A., Bann, K.L., Bhattacharya, J.P., Howell Jr., C.D., 2005. Ichnology of deltas: Organism responses to the dynamic interplay of rivers, waves, storms, and tides. In: Giosan, L., Bhattacharya, J.P. (Eds.), *River Deltas — Concepts, Models, and Examples*. SEPM Special Publications, vol. 83, pp. 49–85. <https://doi.org/10.2110/pec.05.83.0049>.
- Miall, A.D., 1978. Lithofacies types and vertical profile models in braided river deposits: A summary. In: Miall, A.D. (Ed.), *Fluvial Sedimentology*. Canadian Society of Petroleum Geologists, Memoir, vol. 5, pp. 597–604.
- Midtgard, H.H., 1996. Inner-shelf to lower-shoreface hummocky sandstone bodies with evidence for geostrophic influenced combined flow, Lower Cretaceous, West Greenland. *Journal of Sedimentary Research*, 66(2), 343–353.
- Morsilli, M., Pomar, L., 2012. Internal waves vs. surface storm waves: A review on the origin of hummocky cross-stratification. *Terra Nova*, 24(4), 273–282. <https://doi.org/10.1111/j.1365-3121.2012.01070.x>.
- Mount, J., 1985. Mixed siliciclastic and carbonate sediments: A proposed first-order textural and compositional classification. *Sedimentology*, 32(3), 435–442. <https://doi.org/10.1111/j.1365-3091.1985.tb00522.x>.
- Mpodozis, C., Ramos, V., 1989. The Andes of Chile and Argentina. In: Ericksen, G.E., Cañas Pinochet, M.T., Reinemud, J.A. (Eds.), *Geology of the Andes and Its Relation to Hydrocarbon and Mineral Resources: Circum-Pacific Council for Energy and Mineral Resources*. Earth Sciences Series, vol. 11, pp. 59–90 (Houston).
- Mulder, T., Alexander, J., 2001. The physical character of subaqueous sedimentary density flows and their deposits. *Sedimentology*, 48(2), 269–299. <https://doi.org/10.1046/j.1365-3091.2001.00360.x>.
- Mulder, T., Syvitski, J.P.M., 1995. Turbidity currents generated at river mouths during exceptional discharges to the world oceans. *The Journal of Geology*, 103(3), 285–299.
- Mulder, T., Syvitski, J.P.M., Migeon, S., Faugères, J., Savoye, B., 2003. Marine hyperpycnal flows: Initiation, behavior and related deposits. A review. *Marine and Petroleum Geology*, 20(6–8), 861–882. <https://doi.org/10.1016/j.marpetgeo.2003.01.003>.
- Mutti, E., Davoli, G., Tinterri, R., Zavala, C., 1996. The importance of ancient fluvio-deltaic systems dominated by catastrophic flooding in tectonically active basins. *Memorie di Scienze Geologiche, Università di Padova*, 48, 233–291.
- Mutti, E., Gulisano, C.A., Legarreta, L., 1994a. Anomalous systems tracts stacking patterns within third order depositional sequences (Jurassic–Cretaceous Back Arc Neuquén Basin, Argentine Andes). In: *Second High-Resolution Sequence Stratigraphy Conference, Abstracts*, pp. 137–143 (Trempe).
- Mutti, E., Gulisano, C.A., Legarreta, L., 1994b. Flood-related gravity-flow deposits in fluvial and fluvio-deltaic depositional systems and their sequence stratigraphic implications. In: *Second High-Resolution Sequence Stratigraphy Conference, Abstracts*, pp. 131–136 (Trempe).
- Nichols, G., 1999. *Sedimentology and Stratigraphy*. Blackwell, London.
- Omarini, J., Lescano, M., Odino-Barreto, A.L., Campetella, D., Tunik, M., Garbán, G., Brea, F., Erra, G., Aguirre-Urreta, B., Martinez, M., 2020. Palaeoenvironmental conditions for the preservation of organic matter during the late Hauterivian in the Neuquén Basin (Western Argentina). *Marine and Petroleum Geology*, 120, 104469. <https://doi.org/10.1016/j.marpetgeo.2020.104469>.
- Otharín, G., 2020. *Sedimentología y análisis de facies de la Formación Vaca Muerta (Tithoniano-Valanginiense), Cuenca Neuquina. El rol de los flujos de fango en la depositación de espesas sucesiones de lutitas*. Ph.D Thesis. Universidad Nacional del Sur, Bahía Blanca.
- Otharín, G., Zavala, C., Arcuri, M., Di Meglio, M., Zorzano, A., Marchal, D., Köhler, G., 2020. Análisis de facies en depósitos de grano fino asociados a flujos de fango. Formación Vaca Muerta (Tithoniano-Valanginiense), Cuenca Neuquina central, Argentina. *Andean Geology*, 47(2), 384–417.
- Overeem, I., Kroonenberg, S.B., Veldkamp, A., Groenesteijn, K., Rusakov, G.V., Svitoch, A.A., 2003. Small-scale stratigraphy in a large ramp delta: Recent and Holocene sedimentation in the Volga delta, Caspian Sea. *Sedimentary Geology*, 159(3–4), 133–157. [https://doi.org/10.1016/S0037-0738\(02\)00256-7](https://doi.org/10.1016/S0037-0738(02)00256-7).
- Paolillo, M.A., Guler, M.V., Lazo, D.G., Pazos, P.J., Ottone, E.G., Aguirre-Urreta, B., 2018. Early Cretaceous dinoflagellate cysts from the Agrio Formation at its type locality (Neuquén Basin, Argentina) and their biostratigraphic implications. *Ameghiniana*, 55(5), 554–570.
- Pazos, P.J., Lazo, D.G., Tunik, M.A., Marsicano, C.A., Fernández, D.E., Aguirre-Urreta, M.B., 2012. Paleoenvironmental framework of dinosaur tracksites and other ichnofossils in Early Cretaceous mixed siliciclastic-carbonate deposits in the Neuquén Basin, northern Patagonia (Argentina). *Gondwana Research*, 22(3–4), 1125–1140. <https://doi.org/10.1016/j.gr.2012.02.003>.
- Pettijohn, F.J., 1975. *Sedimentary Rocks*. Harper & Row, New York.
- Ponce, J.J., Montagna, A.O., Carmona, N.B., Canale, N., 2015. *Guía de Campo. Escuela de Verano 2015. Sedimentología e Icnología de los Sistemas Petroleros no Convencionales de la Cuenca Neuquina (Los Molles-Lajas y Vaca*

- Muerta-Quintuco). Universidad Nacional de Río Negro-Fundación YPF.
- Postma, G., 1995. Causes of architectural variations in deltas. In: Oti, M.N., Postma, G. (Eds.), *Geology of Deltas*. Balkema, The Netherlands, pp. 3–16.
- Potter, P.E., Maynard, J.B., Depetris, P.J., 2005. *Mud and Mudstones: Introduction and Overview*. Springer, New York.
- Ramos, V.A., Folguera, A., 2005. Tectonic evolution of the Andes of Neuquén: Constraints derived from the magmatic arc and foreland deformation. In: Veiga, G.D., Spalletti, L.A., Howell, J.A., Schwarz, E. (Eds.), *A Case Study in Sequence Stratigraphy and Basin Dynamics*. Geological Society, London, Special Publications, vol. 252, pp. 15–35. <https://doi.org/10.1144/GSL.SP.2005.252.01.02>.
- Ramos, V.A., Kay, S.M., 2006. Overview of the tectonic evolution of the southern central Andes of Mendoza and Neuquén (35°–39°S latitude). In: Kay, S.M., Ramos, V.A. (Eds.), *Evolution of an Andean Margin: A Tectonic and Magmatic View from the Andes to the Neuquén Basin* (35°–39°S lat). GSA Special Papers, vol. 407, pp. 1–17. [https://doi.org/10.1130/2006.2407\(01](https://doi.org/10.1130/2006.2407(01).
- Reineck, H., Wunderlich, F., 1968. Classification and origin of flaser and lenticular bedding. *Sedimentology*, 11(1–2), 99–104. <https://doi.org/10.1111/j.1365-3091.1968.tb00843.x>.
- Sagasti, G., 2005. Hemipelagic record of orbitally-induced dilution cycles in Lower Cretaceous sediments of the Neuquén Basin. In: Veiga, G.D., Spalletti, L.A., Howell, J.A., Schwarz, E. (Eds.), *A Case Study in Sequence Stratigraphy and Basin Dynamics*. Geological Society, London, Special Publications, vol. 252, pp. 231–250. <https://doi.org/10.1144/GSL.SP.2005.252.01.11>.
- Sanders, J.E., 1965. Primary sedimentary structures formed by turbidity currents and related resedimentation mechanisms. In: Middleton, G.V. (Ed.), *Primary Sedimentary Structures and Their Hydrodynamic Interpretation*. SEPM Special Publication, vol. 12, pp. 192–219. <https://doi.org/10.2110/pec.65.08.0192>.
- Schieber, J., Southard, J.B., 2009. Bedload transport of mud by floccule ripples — Direct observation of ripple migration processes and their implications. *Geology*, 37(6), 483–486. <https://doi.org/10.1130/G25319A.1>.
- Schieber, J., Southard, J., Thaisen, K., 2007. Accretion of mudstone beds from migrating floccule ripples. *Science*, 318(5857), 1760–1763. <https://doi.org/10.1126/science.1147001>.
- Schieber, J., Yawar, Z., 2009. A new twist on mud deposition: Mud ripples in experiment and rock record. *The Sedimentary Record*, 7(2), 4–8.
- Simons, D.B., Richardson, E.V., Nordin Jr., C.F., 1965. Sedimentary structures generated by flow in alluvial channels. In: Middleton, G.V. (Ed.), *Primary Sedimentary Structures and Their Hydrodynamic Interpretation*. SEPM Special Publication, vol. 12. SEPM Special Publication, pp. 34–52. <https://doi.org/10.2110/pec.65.08.0034>.
- Soares, J.L., Santos, H.P., Brito, A.S., Nogueira, A.A.E., Nogueira, A.C.R., Amorim, K.B., 2020. The crustaceans burrow *Sinusichnus sinuosus* from the Oligocene–Miocene carbonate deposits of eastern Amazonia. *Ichnos*, 27(2), 97–106. <https://doi.org/10.1080/10420940.2019.1697256>.
- Southard, J.B., 1991. Experimental determination of bed-form stability. *Annual Review of Earth and Planetary Sciences*, 19, 423–455. <https://doi.org/10.1146/annurev.ea.19.050191.002231>.
- Spalletti, L.A., Franzese, J.R., Matheos, S.D., Schwarz, E., 2000. Sequence stratigraphy of a tidally dominated carbonate–siliciclastic ramp; the Tithonian–Early Berriasian of the southern Neuquén Basin, Argentina. *Journal of the Geological Society*, 157(2), 433–446. <https://doi.org/10.1144/jgs.157.2.433>.
- Spalletti, L.A., Poiré, D.G., Pirrie, D., Matheos, S., Doyle, P., 2001a. Respuesta sedimentológica a cambios en el nivel de base en una secuencia mixta clástica–carbonática del Cretácico de la Cuenca Neuquina, Argentina. *Revista de la Sociedad Geológica de España*, 14, 57–74.
- Spalletti, L.A., Poiré, D.G., Schwarz, E., Veiga, G.D., 2001b. Sedimentologic and sequence stratigraphic model of a Neocomian marine carbonate–siliciclastic ramp: Neuquén Basin, Argentina. *Journal of South American Earth Sciences*, 14(6), 609–624. [https://doi.org/10.1016/S0895-9811\(01\)00039-6](https://doi.org/10.1016/S0895-9811(01)00039-6).
- Sumner, E.J., Amy, L.A., Talling, P.J., 2008. Deposit structure and processes of sand deposition from decelerating sediment suspensions. *Journal of Sedimentary Research*, 78(8), 529–547. <https://doi.org/10.2110/jsr.2008.062>.
- Tucker, M.E., Wright, V.P., 1990. *Carbonate Sedimentology*. Blackwell Scientific Publications, Oxford.
- Tunik, M.A., Pazos, P.J., Impicini, A., Lazo, D., Aguirre-Urreta, M.B., 2009. Dolomitized tidal cycles in the Agua de la Mula member of the Agrio Formation (Lower Cretaceous), Neuquén Basin, Argentina. *Latin American Journal of Sedimentology and Basin Analysis*, 16(1), 29–43.
- Tyson, R., 1995. *Sedimentary Organic Matter*. Chapman & Hall, London.
- Uliana, M.A., Biddle, K.T., Cerdan, J., 1989. Mesozoic extension and the formation of Argentine sedimentary basins. In: Tankard, A.J., Balkwill, H.R. (Eds.), *Extensional Tectonics and Stratigraphy of the North Atlantic Margins*. AAPG Memoirs, vol. 46, pp. 599–614. <https://doi.org/10.1306/M46497C39>.
- Van Wagoner, J.C., Mitchum, R.M., Campion, K.M., Rahmanian, V.D., 1990. *Siliciclastic sequence stratigraphy in well logs, cores, and outcrops: Concepts for high-resolution correlation of time and facies*. AAPG Methods in Exploration Series, no. 7: 55 p. + 14 fold-out plates. American Association of Petroleum Geologists, Tulsa.
- Veiga, R., Vergani, G.D., 1993. Depósitos de nivel bajo: Nuevo enfoque sedimentológico y estratigráfico del miembro Avilé en el Norte del Neuquén. Argentina. In: *12° Congreso Geológico Argentino y 2° Congreso de Exploración de Hidrocarburos*, Actas I, pp. 55–65 (Mendoza).
- Vergani, G.D., Tankard, A.J., Belotti, H.J., Welsink, H.J., 1995. Tectonic evolution and paleogeography of the Neuquén Basin, Argentina. In: Tankard, A.J., Suárez Soruco, R., Welsink, H.J. (Eds.), *Petroleum Basins of South America*. AAPG Memoir, vol. 62, pp. 383–402.

- Walker, R.G., Duke, W.L., Leckie, D.A., 1983. Hummocky stratification: Significance of its variable bedding sequences: Discussion and reply: Discussion. *GSA Bulletin*, 94(10), 1245–1249. [https://doi.org/10.1130/0016-7606\(1983\)94<1245:HSSOIV>2.0.CO;2](https://doi.org/10.1130/0016-7606(1983)94<1245:HSSOIV>2.0.CO;2).
- Weaver, C.E., 1931. *Paleontology of the Jurassic and Cretaceous of West Central Argentina*. Memoir University of Washington, vol. 1, 469 p. (Seattle).
- Weaver, C.E., 2020. Paleontology of the Jurassic and Cretaceous of West Central Argentina. *Memoir University of Washington*, vol. 1, 469 p. (Seattle)
- Wilson, R.D., Schieber, J., 2014. Muddy prodeltaic hyperpynites in the lower Genesee Group of central New York, USA: Implications for mud transport in epicontinental seas. *Journal of Sedimentary Research*, 84(10), 866–874. <https://doi.org/10.2110/jsr.2014.70>.
- Wright, L.D., Coleman, J.M., 1973. Variations in morphology of major river deltas as functions of ocean wave and river discharge regimes. *AAPG Bulletin*, 57(2), 370–398. <https://doi.org/10.1306/819A4274-16C5-11D7-8645000102C1865D>.
- Zavala, C., Arcuri, M., Di Meglio, M., Zorzano, A., Otharán, G., Irastorza, A., Torresi, A., 2021. Deltas: A new classification expanding bates's concepts. *Journal of Palaeogeography*, 10(3), 341–355. <https://doi.org/10.1186/s42501-021-00098-w>.
- Zavala, C., Arcuri, M., Gamero, H., Contreras, C., Meglio, M.D., 2011. A genetic facies tract for the analysis of sustained hyperpynal flow deposits. In: Slatt, R.M., Zavala, C. (Eds.), *Sediment Transfer from Shelf to Deep Water - Revisiting the Delivery System*. AAPG Studies in Geology, vol. 61, pp. 31–51. <https://doi.org/10.1306/13271349St613438>.
- Zavala, C., Pan, S.X., 2018. Hyperpynal flows and hyperpynites: Origin and distinctive characteristics. *Lithologic Reservoirs*, 30(1), 1–27.
- Zavala, C., Ponce, J.J., Arcuri, M., Drittanti, D., Freije, H., Asensio, M., 2006. Ancient lacustrine hyperpynites: A depositional model from a case study in the Rayoso Formation (Cretaceous) of west-central Argentina. *Journal of Sedimentary Research*, 76(1), 41–59. <https://doi.org/10.2110/jsr.2006.12>.
- Zuffa, G.G., 1980. Hybrid arenites: Their composition and classification. *Journal of Sedimentary Petrology*, 50(1), 21–29. <https://doi.org/10.1306/212F7950-2B24-11D7-8648000102C1865D>.